

Detecting differentially methylated regions in bisulfite sequencing data using quasi-binomial mixed models with smooth covariate effect estimates

Kaiqiong Zhao^{1,2}, Karim Oualkacha³, Lajmi Lakhel-Chaieb⁴, Aurélie Labbe⁵, Kathleen Klein², Sasha Bernatsky^{6,7}, Marie Hudson^{2,6}, Inés Colmegna^{6,7}, Celia M.T. Greenwood^{1,2,8,9}

¹Department of Epidemiology, Biostatistics and Occupational Health, McGill University

²Lady Davis Institute for Medical Research, Jewish General Hospital

³Département de Mathématiques, Université du Québec à Montréal

⁴Département de Mathématiques et de Statistique, Université Laval

⁵Département des Sciences de la Décision, HEC Montréal

⁶Department of Medicine, McGill University

⁷The Research Institute of the McGill University Health Centre

⁸Department of Human Genetics, McGill University

⁹Gerald Bronfman Department of Oncology, McGill University

January 18, 2021

Abstract

Identifying disease-associated changes in DNA methylation can help to gain a better understanding of disease etiology. Bisulfite sequencing technology allows the generation of methylation profiles at single base of DNA. We previously developed a method for estimating smooth covariate effects and identifying differentially methylated regions (DMRs) from bisulfite sequencing data, which copes with experimental errors and variable read depths; this method utilizes the binomial distribution to characterize the variability in the methylated counts. However, bisulfite sequencing data frequently include low-count integers and can exhibit over or under dispersion relative to the binomial distribution. We present a substantial improvement to our previous work by proposing a quasi-likelihood-based regional testing approach which accounts for multiplicative and additive sources of dispersion. We demonstrate the theoretical properties of the

resulting tests, as well as their marginal and conditional interpretations. Simulations show that the proposed method provides correct inference for smooth covariate effects and captures the major methylation patterns with excellent power.

1 Introduction

Conceptually, the emergence of a disease phenotype is believed to stem from the combined effects of genetic predisposition and environmental exposures (Ober and Vercelli, 2011). A plausible mechanism behind this gene-environment interplay is epigenetic modification, which regulates gene activity through modifications of DNA accessibility. Epigenetics may explain how exposures leave heritable marks on the genome that impact disease susceptibility (Jaenisch and Bird, 2003). Therefore, increased understanding of epigenetic-disease association could lead to novel insights into disease causation and possible therapies (Feinberg, 2007).

The most studied epigenetic mark is DNA methylation, which involves the covalent addition of a methyl group to a cytosine nucleotide. DNA methylation, in the mammalian genomes, occurs predominantly at cytosine-guanine dinucleotides (i.e. CpG sites) (Lister et al., 2009). Methylation of CpG-rich promoters can silence gene expression by preventing transcriptional factor binding to DNA (Choy et al., 2010). More generally, DNA methylation has the potential to activate or repress gene expression, depending on whether the mark inactivates a positive or negative regulatory element (Jones, 1999). Known or suspected drivers behind methylation alterations include genetic variations (McRae et al., 2014), environmental toxins (Hanson and Gluckman, 2008), external stressors (Dolinoy et al., 2007) and aging (Horvath, 2013). There is also evidence that localized abnormal methylation is strongly linked to many diseases, including breast cancer (Hu et al., 2005), autism spectrum disorder (Dunaway et al., 2016), and systemic autoimmune disease (Kato et al., 2005).

High-resolution, large-scale measurement of DNA methylation is now possible with recent advances in bisulfite sequencing (BS-seq) protocol, which is implemented either genome-wide or in targeted regions. Although whole-genome bisulfite sequencing (WGBS) allows a comprehensive characterization of the methylation landscape, it is inefficient for large-scale studies as only 20% or less of CpGs are thought to have variable methylation across individuals or tissues (Ziller et al., 2013). On the other

hand, Targeted Custom Capture Bisulfite Sequencing (TCCBS) platform enables a comprehensive yet cost-effective interrogation of functional CpGs in disease-targeted tissues or cells (Allum et al., 2015). This approach has been successfully used to identify novel disease-associated epigenetic variants (Shao et al., 2019; Allum et al., 2019; Ziller et al., 2016). In this work, we aim to improve sensitivity to detect, among all the regions targeted by TCCBS, differentially methylated regions (DMRs) that are associated with phenotypes or traits.

Like other sequencing experiments, the raw data from TCCBS are short sequence reads. After proper alignment and data processing, the methylation level at a single cytosine can be summarized as a pair of counts: the number of methylated reads and the total number of reads covering the site, i.e. read depth. Such data possess several challenges for statistical analysis. Typically, read depth varies drastically across sites and individuals, which leads to measures with wide-ranging precision and many missing values (Sims et al., 2014). Additional statistical challenges are created by the strong spatial correlations observed in methylation levels at neighboring CpG sites (Hansen et al., 2012; Rackham et al., 2017; Korthauer et al., 2018; Shokoohi et al., 2018), as well as the possibility of data errors, arising from excessive or insufficient bisulfite treatment or other aspects of the sequencing processes (Cheng and Zhu, 2013; Lakhali-Chaieb et al., 2017). Furthermore, in addition to the trait of interest (e.g. disease or treatment group), other factors, such as age (Horvath, 2013), batch effects (Leek et al., 2010), or cell-type mixture proportions (for mixed tissue samples) (McGregor et al., 2016) have effects on methylation levels. Hence, it is desirable to adjust methylation signals for multiple covariates simultaneously.

To detect truly differentially methylated regions without finding false associations, it is crucial to accurately account for the sources of variability across individuals. We ran into this issue in a recent analysis of methylation profiles and anti-citrullated protein antibodies (ACPA). Figure 1 (A) illustrates methylation proportions in a targeted region for samples from this study. (A full description of the study, referred to as the ACPA dataset, is in Section 2.2). Clearly, dispersion is much larger between samples in the blue group. In panel (C), it can be seen that p-values testing for methylation differences, assuming a binomial mean-variance relationship are much too small. In contrast, allowing for dispersion through a quasi-binomial model provides p-values in line with null expectation for this region. As such, the restrictive mean-variance relationship implied by a binomial generalized linear model (GLM) may not

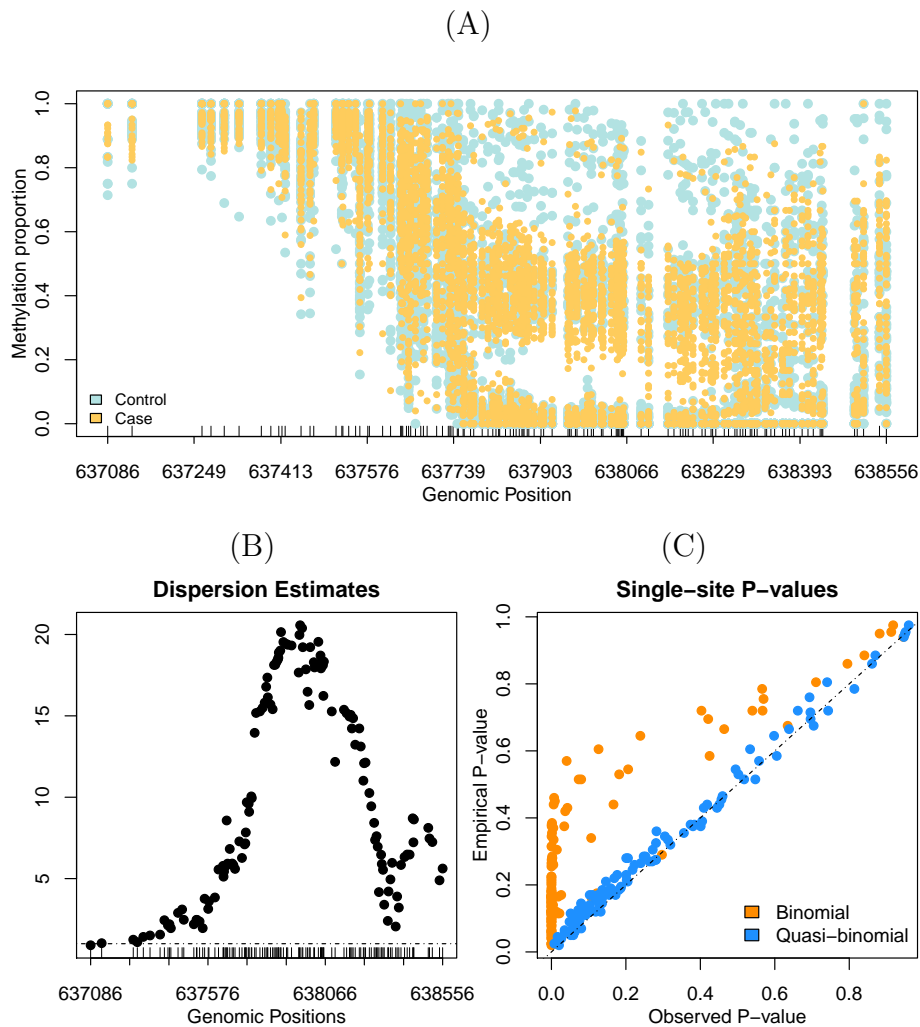


Figure 1. *Illustration of observed dispersion in a targeted region that underwent bisulfite sequencing.* (A) Observed methylation proportions in one region for two groups of samples (yellow and blue); data are fully described in Section 2.2. (B) Estimated dispersion for each CpG site from a single-site quasi-binomial GLM. (C) Single-site p-values for methylation difference between the two groups. Horizontal axis are the p-values estimated from either binomial (ignoring dispersion) or quasi-binomial (accounting for dispersion) GLMs. Vertical axis shows the empirical p-values computed from 199 permutations; the empirical p-value is a benchmark for valid statistical tests. (Single-site beta-binomial regression models generate similar dispersion estimate pattern and p-value distribution to quasi-binomial GLM).

adequately accommodate the data variability, and thus can lead to inflation of false positives. This is known as over or underdispersion, i.e. data presenting greater or

lower variability than assumed by a GLM model.

Moving in this direction, we have developed a SmOoth ModeliNg of BisUlfinite Sequencing (SOMNiBUS) method to detect DMRs in targeted bisulfite sequencing data (Zhao et al., 2020). The method provides a general framework of analysis, and simultaneously addresses regional testing, estimation of multiple covariate effects, adjustment for read depth variability and experimental errors. Specifically, Zhao et al. (2020) proposed a hierarchical binomial regression model, which allows covariate effects to vary smoothly along genomic position. A salient feature of SOMNiBUS is its one-stage nature. Several existing methods first smooth methylation data and then, in a second stage, estimate covariate effects based on the smoothed data (Hansen et al., 2012; Lakhal-Chaieb et al., 2017; Hebestreit et al., 2013), and this two-stage framework could lead to biased uncertainty estimates. In contrast, SOMNiBUS collapses smoothing and testing steps into a single step, and achieves accurate statistical uncertainty assessment of DMRs. That said, its underlying binomial assumption may be overly restrictive and is only applicable when data exhibit variability levels that are similar to those anticipated based on a binomial distribution (such as data from inbred animal or cell line experiments). In this work, we propose an extension of SOMNiBUS, which maintains all the good properties of the standard SOMNiBUS, and at the same time explicitly allows the variability in regional methylation counts to exceed or fall short of what binomial model permits.

The importance of accounting for dispersion in BS-seq data has been well recognized in analysis of single CpG sites. Faced with dispersion in discrete data analysis, one commonly used option is to convert the methylated and total counts to proportions. In this way, testing of differentially methylated single CpG sites can be done via the two sample t-test (Hansen et al., 2012) or beta regression (Hebestreit et al., 2013), both of which allow direct computation of (within-group) sample variation. However, this conversion loses information, since it fails to distinguish between noisy and accurate measurements (Wu et al., 2015), often as a consequence of the stochasticity of read depth, and also disregards the discrete nature of the data (Lea et al., 2015). On the other hand, there are approaches for DNA methylation analysis that directly model counts while accounting for dispersion. These count-based approaches use either *additive* overdispersion models, or *multiplicative* under- or overdispersion models to describe the variation driving the dispersion (Browne et al., 2005). In a multiplicative model, one includes a multiplicative scale factor, i.e. the dispersion

parameter, in the variance of the binomial response. Thus, the dispersion inflates or deflates the variance estimates of the covariate effect by the multiplicative factor. Such approaches include the quasi-binomial regression model (Akalin et al., 2012) and the beta-binomial regression model (Dolzhenko and Smith, 2014; Feng et al., 2014; Park et al., 2014; Park and Wu, 2016). In contrast, additive overdispersion methods add a subject-level random effect (RE) to capture the extra-binomial variation among individual observations. Both ABBA (Rackham et al., 2017) and MACAU (Lea et al., 2015), that use binomial mixed effect models fall in this category. An advantage of the multiplicative approach, particularly the quasi-binomial model, is that it naturally allows for both overdispersion and underdispersion, whereas the additive model only allows overdispersion. On the other hand, the additive overdispersion approach links directly with a multilevel model and can be readily extended to analyze data with a hierarchical or clustering structure.

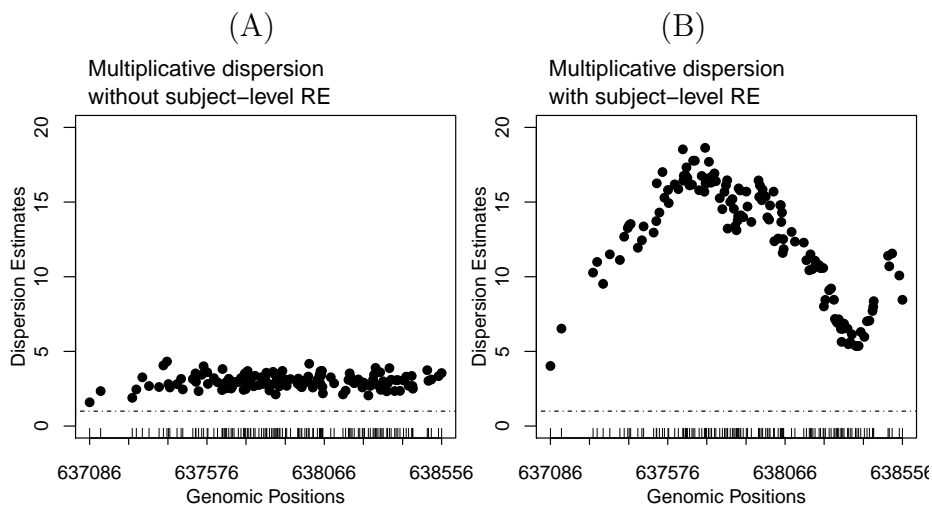


Figure 2. A byproduct of introducing a subject-level RE, on top of a multiplicative dispersion parameter, to a model with smooth covariate effects is a regional dispersion pattern of varying degree. Estimated dispersion for each CpG site obtained from a single-site quasi-binomial GLM, for two simulated regional methylation datasets: (A) data were simulated from a multiplicative-dispersion-only model ($\phi = 3, \sigma_0^2 = 0$), and (B) data were simulated from a model with both a multiplicative dispersion and a subject-level RE ($\phi = 3, \sigma_0^2 = 3$); see Section 2.1 for detailed model formulations and notation definitions.

The challenge of accounting for dispersion when detecting DMRs is further complicated by several factors. Firstly, even within a small genomic region, different CpG

sites may exhibit different levels of dispersion and strong spatial correlation (Figure 1 B). Hence, a multiplicative dispersion model with a common dispersion parameter does not adequately capture the dispersion heterogeneity across loci (Figure 2 A). In addition, challenges are presented by the complex correlation structure in the regional methylation data. Apart from the spatial correlations among neighboring CpGs, there are additional correlations among methylation measurements on the same subject. Ignoring this within-subject correlation could lead to overestimation of precision and invalid statistical tests (Cui et al., 2016). One means to accommodate such a correlation structure is to add a subject-level RE that can also capture the overdispersion induced by independent variation across different subjects. Furthermore, when modeling discrete data with a hierarchical structure, extra non-structural specific random dispersion can arise, beyond that introduced by the subject-level RE (Breslow and Clayton, 1993; Molenberghs et al., 2007; Vahabi et al., 2019), and thus, often, parametric distributions with restrictive mean-variance relations poorly describe the outcomes for individual subjects (i.e. the conditional distribution of outcome given the RE) (Molenberghs et al., 2010, 2012; Ivanova et al., 2014). Hence, properly addressing both multiplicative and additive sources of dispersion in methylation data is essential for making reliable inference at the region level.

Table 1. List of existing DNA methylation analytical methods and our proposal with their capabilities.

Method	regional	one-stage	count-based	read-depth variability	adjust for confounding	within-subject correlation	non-structural dispersion	varying levels of dispersion across loci	experimental errors
dSOMNiBUS	✓	✓	✓	✓	✓	✓	✓	✓	✓
SOMNiBUS	✓	✓	✓	✓	✓				✓
BSmooth	✓			✓			✓	✓	
SMSC	✓			✓			✓	✓	✓
dmrseq	✓	✓		✓	✓	✓	✓		
Biseq	✓			✓	✓	✓	✓	✓	
GlobalTest	✓	✓			✓	NA [†]	NA [†]	NA [†]	
ABBA	✓	✓	✓	✓		✓	✓	✓	
MACAU		✓	✓	✓	✓	NA [‡]	✓	✓	

✓: These three methods are of a two-stage nature. Their smoothing stage indeed accounts for read-depth variability, but their testing stage, which relies on t-test or beta regression, ignores the read-depth variability.

†: GlobalTest treats methylation levels at multiple loci as covariates and trait of interest as outcome. It is not necessary for GlobalTest to account for the three features on covariance structure of methylation across samples and loci.

‡: MACAU is a single-site method and within-subject correlation is irrelevant when analyzing individual sites one at a time.

Given our preliminary exploration of dispersion in the ACPA dataset, we recognized the need for a regional one-stage method of analysis that accommodates both the hierarchically-induced overdispersion (and/or correlation) and the extra unstructured individual dispersion. This desired method should also simultaneously address discrete nature of the data, varying strength of dispersion across a region, estimation of multiple covariate effects, adjustment for read depth variability and experimental errors. However, to the best of our knowledge, none of the existing methods meet all aforementioned objectives (Table 1). For example, dmrseq (Korthauer et al., 2018), which fits a generalized least squares regression model with autoregressive error structure to the transformed methylation proportions, accommodates both within-subject correlation and non-structural dispersion, but it assumes a constant dispersion parameter for all loci in a region. Biseq (Hebestreit et al., 2013) is capable of capturing the covariance structure of regional methylation data (by estimating the variogram of site-specific test statistics). However, this method separates smoothing and inference steps and its final significance assessment does not account for the uncertainty in the smoothing step.

To overcome the limitations and challenges of existing methods, we propose a novel approach for identifying DMRs, dSOMNiBUS (dispersion-adjusted SmOoth ModeliNg of BisUlfitE Sequencing). Our strategy directly models raw read counts while accounting for all (known) sources of data variability and varying degree of dispersion across loci, thus providing accurate assessments of regional statistical significance.

Specifically, we propose a quasi-binomial mixed model to describe bisulfite sequencing data, which allows covariate effects to vary smoothly along genomic positions, and specially, captures the extra-binomial variation by the *combination* of a subject-specific RE (i.e an additive overdispersion) and a multiplicative dispersion. The RE term accounts for between-sample heterogeneity, and at the same time enables flexible dispersion patterns in a region (Figure 2 B), which is highly plausible in methylation data (Figure 1 B). The multiplicative dispersion, on the other hand, explicitly allows the variability in individual subject’s methylation levels to exceed or fall short of what binomial distribution assumes, and thus captures the extra dispersion that cannot explained by RE. In addition, our approach accounts for possible data errors in the observed methylated counts. Specifically, we assume that the observed read counts arise from an unobserved latent true methylation state compounded by errors. We then build a specialized expectation-maximization (EM) algorithm for the

quasi-binomial mixed model to make inference about DMRs in the presence of data errors.

2 Results

2.1 The smoothed quasi-binomial mixed model

Here we present our model for describing regional methylation data. Details on the algorithm, and the inference method for the model, are provided in Section 4.

We consider DNA methylation measures over a targeted genomic region from N independent samples. Let m_i be the number of CpG sites for the i^{th} sample, $i = 1, 2, \dots, N$. We write t_{ij} for the genomic position (in base pairs) for the i^{th} sample at the j^{th} CpG site, $j = 1, 2, \dots, m_i$. Methylation levels at a site are quantified by the number of methylated reads and the total number of reads. We define X_{ij} as the total number of reads aligned to CpG j from sample i . We denote the *true* methylation status for the k^{th} read obtained at CpG j of sample i as S_{ijk} , where $k = 1, 2, \dots, X_{ij}$. For a single DNA strand read, S_{ijk} is binary and we define $S_{ijk} = 1$ if the corresponding read is methylated and $S_{ijk} = 0$ otherwise. We additionally denote the *true* methylated counts at CpG j for sample i with $S_{ij} = \sum_{k=1}^{X_{ij}} S_{ijk}$, summing over all reads aligned to position t_{ij} . Furthermore, we assume that we have the information on P covariates for the N samples, denoted as $\mathbf{Z}_i = (Z_{1i}, Z_{2i}, \dots, Z_{Pi})$, for $i = 1, 2, \dots, N$.

We propose a quasi-binomial mixed effect model to describe the relationship between methylated counts, S_{ij} for $j = 1, 2, \dots, m_i$, and the sample-level covariates \mathbf{Z}_i . Specifically,

$$\log \frac{\pi_{ij}}{1 - \pi_{ij}} = \beta_0(t_{ij}) + \beta_1(t_{ij})Z_{1i} + \beta_2(t_{ij})Z_{2i} + \dots + \beta_P(t_{ij})Z_{Pi} + u_i, \quad (1)$$

$$u_i \stackrel{iid}{\sim} N(0, \sigma_0^2)$$

$$\text{Var}(S_{ij} | u_i) = \phi X_{ij} \pi_{ij} (1 - \pi_{ij}) \quad (2)$$

where $\pi_{ij} = \mathbb{E}(S_{ij} | u_i) / X_{ij}$ is the *individual's* methylation proportion (i.e. the conditional mean), $\beta_0(t_{ij})$ and $\{\beta_p(t_{ij})\}_{p=1}^P$ are functional parameters for the intercept and covariate effects on π_{ij} , and σ_0^2 is the random effect variance. In this model, we assume the underlying proportion of methylated reads for the i^{th} sample at the

j^{th} CpG site, π_{ij} , depends on covariates \mathbf{Z}_i and on nearby methylation patterns through a logit link function. In addition, each π_{ij} incorporates a subject-specific random intercept (i.e. an additive overdispersion) u_i that is normally distributed and independent across samples. The inclusion of u_i allows for sample heterogeneity in baseline methylation patterns, and at the same time accounts for the correlation among methylation measurements taken on the same sample. Moreover, we assume the variance of S_{ij} for individual samples to be a product of a multiplicative dispersion parameter ϕ and a known mean-variance function implied by a binomial distribution ($V(\pi_{ij}) = X_{ij}\pi_{ij}(1 - \pi_{ij})$).

Both the random effects $\mathbf{u} = (u_1, u_1, \dots, u_N)^T$ and the multiplicative dispersion parameter ϕ capture extra-binomial dispersion. However, they address two different aspects of dispersion: \mathbf{u} models the variation that is due to independent noise across samples, while ϕ aims to relax the assumption of the conditional distribution of S_{ij} given \mathbf{u} such that it is not confined to a binomial distribution. In fact, our model generalizes the binomial-based model in Zhao et al. (2020) by introducing both the additive dispersion term \mathbf{u} and multiplicative dispersion term ϕ . Specially, imposing $\phi = 1$ in model (1) leads to an additive-dispersion-only model and $\sigma_0^2 = 0$ corresponds to a multiplicative-dispersion-only model. When $\sigma_0^2 = 0$ and $\phi = 1$, our model reduces to the binomial-based model in Zhao et al. (2020).

2.1.1 Marginal interpretations

A key feature of the mixed effect model in (1) is that the regression coefficients $\beta_p(t_{ij})$ need to be interpreted conditional on the value of random effect u_i . For example, $\beta_p(t_{ij})$ describes how an *individual's* methylation proportions in a region depend on covariate Z_p . If one desires estimates of such covariate effects on the average population, it is more appropriate to determine the marginal model implied by (1). After applying a cumulative Gaussian approximation to the logistic function and taking an expectation over u_i , it can be shown that the marginal mean, π_{ij}^M , has the form

$$\pi_{ij}^M = \mathbb{E}(S_{ij})/X_{ij} \approx g\left(\sum_{p=0}^P a \beta_p(t_{ij})Z_{pi}\right), \quad (3)$$

where $g(x) = 1/(1 + \exp(-x))$, $Z_{0i} \equiv 1$, and the constant $a = (1 + c^2\sigma_0^2)^{-1/2}$ with $c = \sqrt{3.41}/\pi$; see detailed derivations in Appendix A.1. The approximation in (3)

is quite accurate with errors ≤ 0.001 . Thus, the marginal mean induced by our mixed effect model depends on the covariates Z_p through a logistic link with attenuated regression coefficients $a\beta_p(t_{ij})$. Although the smooth covariate effect parameters $\beta_p(t_{ij})$ have no marginal interpretation, they do have a strong relationship to their marginal counterparts. Hence, the results from hypothesis testing $H_0 : \beta_p(t_{ij}) = 0$ describe the significance of the covariate effect on both the population-averaged and an individual's DNA methylation levels across a region.

Similarly, the marginal variance of S_{ij} does not coincide with its conditional counterpart as shown in (2). Specifically, our mixed effect model implies a marginal variance of S_{ij} defined as

$$\begin{aligned} \text{Var}(S_{ij}) \approx & X_{ij}\pi_{ij}^*(1 - \pi_{ij}^*) \{ \phi + \sigma_0^2 (X_{ij} - \phi) \pi_{ij}^*(1 - \pi_{ij}^*) \\ & + \sigma_0^2/2(1 - 2\pi_{ij}^*)^2 [1 + \sigma_0^2\pi_{ij}^*(1 - \pi_{ij}^*)(X_{ij} - \phi - 1/2)] \}, \end{aligned} \quad (4)$$

where $\pi_{ij}^* = g^{-1} \left(\sum_{p=0}^P \beta_p(t_{ij}) Z_{pi} \right)$; see detailed derivations in Appendix A.2. Note that π_{ij}^* is the mean methylation proportion when setting random effects u_i to zero and is related to the marginal mean π_{ij}^M via $\pi_{ij}^* = g \left(g^{-1} (\pi_{ij}^M) / a \right)$. Equation (4) illustrates that, under the dSOMNiBUS model, the marginal variance of methylated counts at a CpG site is approximately the variance of the binomial model multiplied by a dispersion factor $\phi^* = \phi + \sigma_0^2 (X_{ij} - \phi) \pi_{ij}^*(1 - \pi_{ij}^*) + \sigma_0^2/2(1 - 2\pi_{ij}^*)^2 [1 + \sigma_0^2\pi_{ij}^*(1 - \pi_{ij}^*)(X_{ij} - \phi - 1/2)]$, which depends on the combined effect of ϕ , the multiplicative dispersion for the conditional variance given the RE, and σ_0^2 , the variance of the subject-level RE. Notably, the marginal dispersion factor ϕ^* also depends on genomic position t_{ij} via the dependence of π_{ij}^* on t_{ij} . Consequently, our dSOMNiBUS model in (1) naturally allows dispersion levels to vary across loci, whereas a multiplicative-dispersion-only model (i.e. $\sigma_0^2 = 0$) can only accommodate constant dispersion in a region, as illustrated in Figure 2. It is also clear from Equation (4) that an additive-dispersion-only model (i.e., $\phi = 1$) only allows for overdispersion, and the combination of additive and multiplicative dispersion naturally accounts for both over- and underdispersion.

2.1.2 Dealing with possible measurement errors in methylated counts

In the presence of experimental errors, the true methylation data, S_{ij} are unknown and one only observes Y_{ij} . We assume the following error mechanism

$$\begin{aligned} P(Y_{ijk} = 1 \mid S_{ijk} = 0) &= p_0 \\ P(Y_{ijk} = 1 \mid S_{ijk} = 1) &= p_1. \end{aligned} \tag{5}$$

Here, these two parameters capture errors; p_0 is the rate of false methylation calls, and $1 - p_1$ is the rate of false non-methylation calls. These rates are assumed to be constant across all reads and positions. The error parameters p_0 and p_1 can be estimated by looking at raw sequencing data at CpG sites known in advance to be methylated or unmethylated (Wreczycka et al., 2017). We assume hereafter that p_0 and p_1 are known. The methodology details on how to make inference about covariate effects $\beta_p(t_{ij})$ and estimate dispersion parameters ϕ and σ_0^2 , in the presence of data errors, are described in Section 4.3.

2.2 Illustration of performance of dSOMNiBUS in the ACPA dataset

We first apply our approach to targeted bisulfite sequencing data from a rheumatoid arthritis study (Shao et al., 2019). Participants were sampled from the CARTaGENE cohort (<https://www.cartagene.qc.ca/>), a population-based cohort including 43,000 general population subjects aged 40 to 69 years in Quebec, Canada. The study aims to investigate association between DNA methylation and the levels of anti-citrullinated protein antibodies (ACPA), a marker of rheumatoid arthritis (RA) risk that often presents prior to any clinical manifestations (Forslind et al., 2004).

Firstly, the serum ACPA levels were measured for a randomly sampled 3600 individuals from the CARTaGENE cohort, based upon which individuals were classified as either ACPA positive or ACPA negative. Then, the whole blood samples of the ACPA positive individuals, and a selected subset of age-sex-and-smoking-status-matched ACPA negative individuals were sent for Targeted Custom Capture Bisulfite Sequencing. Specifically, the sequencing used an immune targeted panel that covers the majority of genomic regions with relevance to RA and blood cells. Cell type proportions in the blood samples were also measured at the time of the sampling (Shao

et al., 2019).

Using this sampling approach, two batches of data, referred to as data 1 and data 2, were collected in 2017 and 2019, respectively. Notably, the classification criteria for ACPA status are slightly different between data 1 and 2. When sampling data 1, subjects with serum ACPA levels greater than 20 optical density (OD) units were called as ACPA positive and samples with ACPA levels less than 20 OD were defined as ACPA negative. After data cleaning, data 1 consisted of 69 ACPA positive subjects and 68 ACPA negative subjects. In contrast, the sampling of data 2 was based on more extreme cutoffs for ACPA levels, and resulted in 60 ACPA positive subjects (ACPA levels ≥ 60 OD) and 60 ACPA negative subjects (ACPA levels < 20 OD). This change in decision is reflected in the different distributions of serum ACPA levels between data 1 and 2, as shown in Supplementary Figure S1. Average sequence read depths in targeted regions were 5 and 35 in data 1 and 2, respectively (Supplementary Figure S2), due to improvement in the sequencing protocols implemented between the two experiments.

In this article, we restricted our attention to regions with at least 50 CpG sites. In addition, we excluded regions with more than 95% CpGs having median read depth 0 or having median methylation proportion as 0. Overall, we analyzed 10,759 regions in dataset 1 and 12,983 regions in dataset 2. We excluded the samples who reported a diagnosis of RA before the CARTaGENE study started. Subjects with missing information on cell type proportions were also removed from our analysis. Supplementary Table S1 presents the sample characteristics in data 1 and 2.

We apply our approach to both data 1 and 2, with the aim to identify the differentially methylated regions that show association with ACPA, after adjustment for age, sex, smoking status and cell type composition. Specifically, we assumed no data errors in the datasets ($p_0 = 1 - p_1 = 0$). We used natural cubic splines to expand the smooth terms in the model, and its rank L_p was approximately as the number of CpGs in a region divided by 10 for $\beta_0(t)$, and divided by 20 for $\beta_p(t), p \geq 1$.

2.2.1 Both additive and multiplicative dispersion is present in the data

Figure 3 presents the distribution of estimated multiplicative dispersion ϕ and additive dispersion σ_0^2 for all test regions in dataset 1 and 2. Overall, widespread overdispersion is observed; 98.5% regions show multiplicative dispersion ϕ greater than 1 and

51.2% regions show additive dispersion σ_0^2 greater than 0.05. The Pearson correlation coefficient between the estimated ϕ and σ_0^2 is -0.015 . There exist 49.8% regions with both multiplicative dispersion $\phi > 1$ and additive dispersion $\sigma_0^2 > 0.05$.

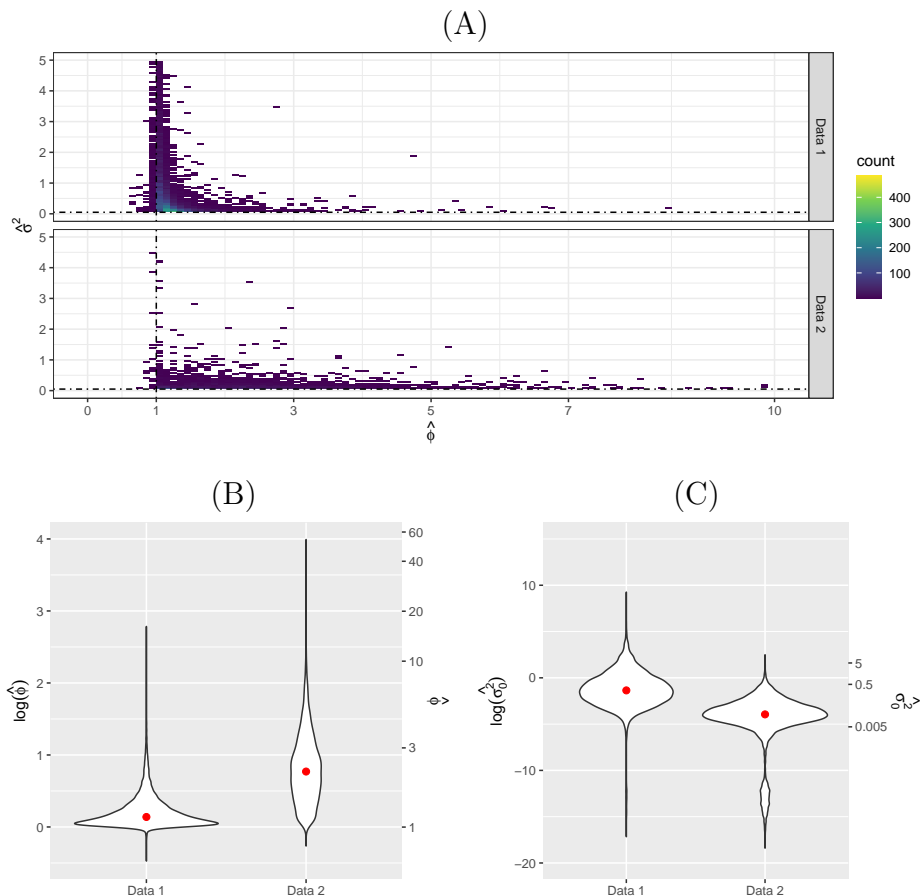


Figure 3. Distribution of the estimated multiplicative dispersion parameter $\hat{\phi}$ and additive dispersion parameter $\hat{\sigma}_0^2$, for all test regions in dataset 1 and 2. Panel (A) shows the 2-dimensional histogram for $\hat{\phi}$ and $\hat{\sigma}_0^2$, where the color intensity represents the number of regions with a particular combination of values of $\hat{\phi}$ and $\hat{\sigma}_0^2$. Panels (B) and (C) show the rotated kernel density plots (i.e. violin plots) for $\hat{\phi}$ and $\hat{\sigma}_0^2$ (in a natural logarithmic scale), separately.

2.2.2 Ignoring either type of dispersion leads to inflated type I errors

Figure 4 shows quantile-quantile (QQ) plots for the regional p-values for the effect of ACPA on the 292 regions of Chromosome 18 in the two datasets. Detailed inference steps are given in Section 4. The results are compared among four different

approaches: (1) dSOMNiBUS which models both the multiplicative and additive dispersion, (2) the multiplicative-dispersion-only model, (3) the additive-dispersion-only model, and (4) the standard SOMNiBUS which ignores any extra-binomial variation. Figure 4 reveals that, when ignoring either type of dispersion, the distribution of regional p-values is biased away from what would be expected under the null. The inclusion of both multiplicative and additive dispersion is important for correct type I error control.

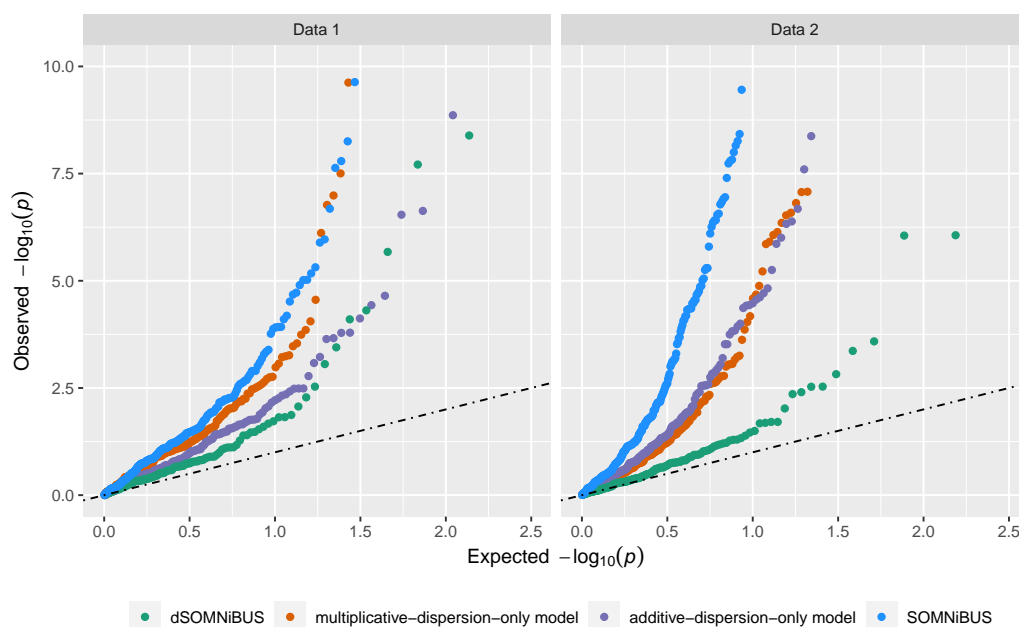


Figure 4. QQ plot for regional p-values, obtained from models addressing different types of dispersion.

2.2.3 Our inference procedure provides well-calibrated p-values

To test DMRs, we propose a region-based statistic with a F limiting distribution; see details in Section 4.4.3. To test the validity of our inference, we compare our regional p-values to bootstrap-based p-values, whose null distribution is constructed by parametric bootstraps (Davison and Hinkley, 1997) and does not rely on any distributional assumptions. Figure 5 shows the distributions of bootstrap-based and our analytical p-values for the targeted regions on chromosome 18, demonstrating that our inference method generates p-values in line with the bootstrap-based results. Thus, dSOMNiBUS provides accurate tests for DMRs without requiring extensive

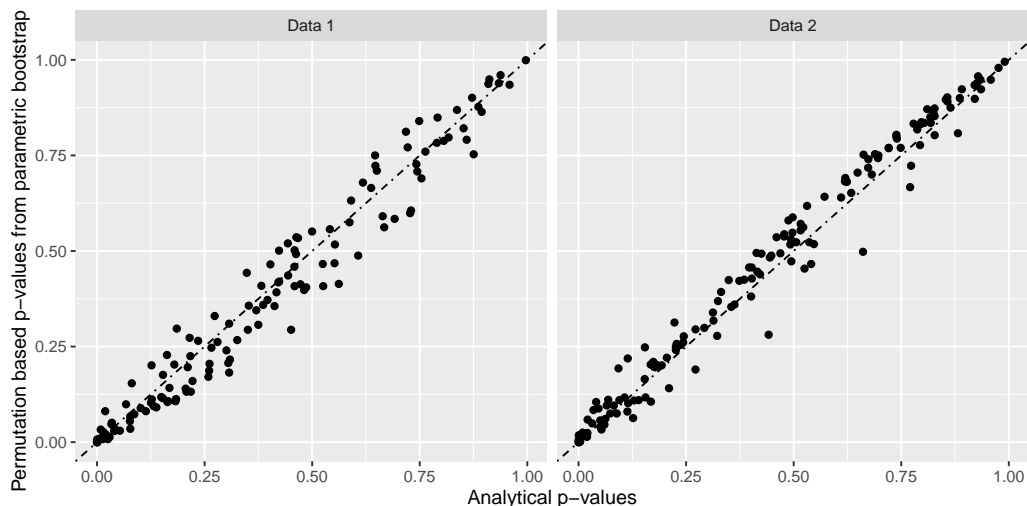


Figure 5. Comparison between the observed regional p values from our approach and the permutation-based p values from parametric bootstrap.

computational time.

2.3 Simulation study

We conducted simulations to assess the proposed inference of smooth covariate effects, and to compare the performance of our method with five existing methods: BiSeq (Hebestreit et al., 2013), BSmooth (Hansen et al., 2012), SMSC (Lakhal-Chaieb et al., 2017), dmrseq (Korthauer et al., 2018) and GlobalTest (Goeman et al., 2006), in terms of type I error and power. Detailed descriptions of these five methods are given in Supplementary Section 3.2. We also made special modifications for the implementations of BSmooth, SMSC and dmrseq, which are primarily designed for WGBS data, to make them as appropriate as possible for targeted regions. see details in Supplementary Section 3.1.

2.3.1 Simulation design

We adopt similar simulation parameters as described in Zhao et al. (2020), and simulated methylation regions with 123 CpG sites under various settings. We first generated the read depth X_{ij} by adding Bernoulli random variables (with proportion 0.5) to a pre-specified regional read-depth pattern (Supplementary Figure S3). In this way, the spatial correlation of read depth observed in real data was well preserved in

the simulated data. The rest of simulation parameters were defined in Table 2.

Table 2. Simulation settings for the functional parameters $\beta_p(t)$, sample size N , error parameters p_0 and p_1 , multiplicative parameter ϕ and RE variances σ_0^2 .

Simulation parameters	Possible values
$\beta_p(t)$	Scenario 1: three covariates: $Z_1 \sim \text{Bernoulli}(0.51)$, $Z_2 \sim \text{Bernoulli}(0.58)$ and $Z_3 \sim \text{Bernoulli}(0.5)$ with effects $\beta_1(t)$, $\beta_2(t)$ and $\beta_3(t)$ and intercept $\beta_0(t)$, shown in the red curves in Figure 7. Here, Z_3 is the null covariate with effect $\beta_3(t) \equiv 0$. Scenario 2: one covariate: $Z \sim \text{Bernoulli}(0.5)$ with 15 different settings of $(\beta_0(t), \beta_1(t))$, which yield methylation proportion parameters as depicted in Figure 6.
N	100
(p_0, p_1)	$(0.003, 0.9)^\dagger$ or $(0, 1)$
ϕ	$(1, 3)$
σ_0^2	$(0, 1, 3, 9)$, and the corresponding subject-specific RE $u_i \stackrel{i.i.d}{\sim} N(0, \sigma_0^2)$ for $i = 1, 2, \dots, N$

\dagger the value 0.003 was reported by Prochenka et al. (2015) as insufficient Bisulfite conversion rate and 0.1 was estimated as the average excessive conversion rate from a (single-cell-type) bisulfite dataset in Hudson et al. (2017) using the method SMSC (Lakhali-Chaieb et al., 2017).

Simulate dispersed-binomial counts. Given the values of $\{Z_1, \dots, Z_P\}$, $\{\beta_p(t), p = 0, 1, \dots, P\}$ and $\{u_i, i = 1, 2, \dots, N\}$ under each setting, the individual’s methylation proportion, π_{ij} , can be readily calculated from the mean model in (1). We then generated the true methylation counts S_{ij} from a beta-binomial distribution with proportion parameter $\mu = \pi_{ij}$, correlation parameter $\rho = \frac{\phi - 1}{X_{ij} - 1}$, and size parameter $n = X_{ij}$. Specifically, S_{ij} were drawn from the following probability mass function

$$P(S_{ij} = k \mid \mu, \rho, n) = \binom{n}{k} \frac{B(k + \alpha, n - k + \beta)}{B(\alpha, \beta)}$$

where $\alpha = \mu(1 - \rho)/\rho$, $\beta = (1 - \mu)(1 - \rho)(1 - \mu)/\rho$, and $B(\cdot, \cdot)$ is the beta function. The variance of S_{ij} can be thus derived as

$$\text{Var}(S_{ij}) = [1 + (n - 1)\rho] [n\mu(1 - \mu)] = \phi X_{ij} \pi_{ij} (1 - \pi_{ij}),$$

which coincides with our assumed mean-variance relationship in (2). We then generated the observed methylated counts Y_{ij} according to the error model in (5), which implies

$$Y_{ij} \mid S_{ij} \sim \text{Binomial}(S_{ij}, p_1) + \text{Binomial}(X_{ij} - S_{ij}, p_0).$$

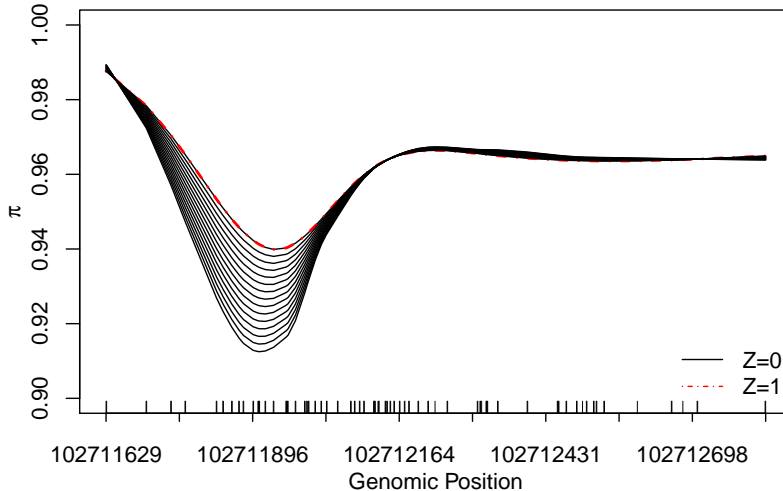


Figure 6. The 15 simulation settings of methylation parameters $\pi_0(t)$ and $\pi_1(t)$ in Scenario 2. Here, $\pi_0(t)$ and $\pi_1(t)$ denote the methylation parameters for samples with $Z = 0$ and $Z = 1$ at position t , respectively. Under this scenario, $\pi_1(t)$ (red dotted-dashed curve) is fixed across settings, whereas $\pi_0(t)$ s (black solid lines) vary across settings corresponding to different degrees of closeness between methylation patterns in the two groups.

Under each scenario and setting, we generated data sets with sample sizes $N = 100$, each 1000 times. We then applied `dSOMNiBUS` along with methods `BiSeq`, `dmrseq`, `BSmooth`, `SMSC` and `GlobalTest` to the simulated data sets. For our approach `dSOMNiBUS`, we used cubic splines with dimension $L_p = 5$ to parameterize the smooth terms of interest. We also assumed that the correct values of error parameters p_0 and p_1 were known.

2.3.2 `dSOMNiBUS` provides accurate inference for smooth covariate effects

Figure 7 presents the estimates of the functional parameters $\beta_0(t)$, $\beta_1(t)$, $\beta_2(t)$ and $\beta_3(t)$ over 1000 simulations, obtained from `dSOMNiBUS`; here, data were generated under Scenario 1, with multiplicative dispersion parameter $\phi = 3$, RE variance $\sigma_0^2 = 3$, and error parameters $p_0 = 0.003$ and $1 - p_1 = 0.1$. Figure 7 demonstrates that the proposed method provides unbiased curve estimates for smooth covariate effects when the regional methylation counts exhibit extra-parametric variation and are measured

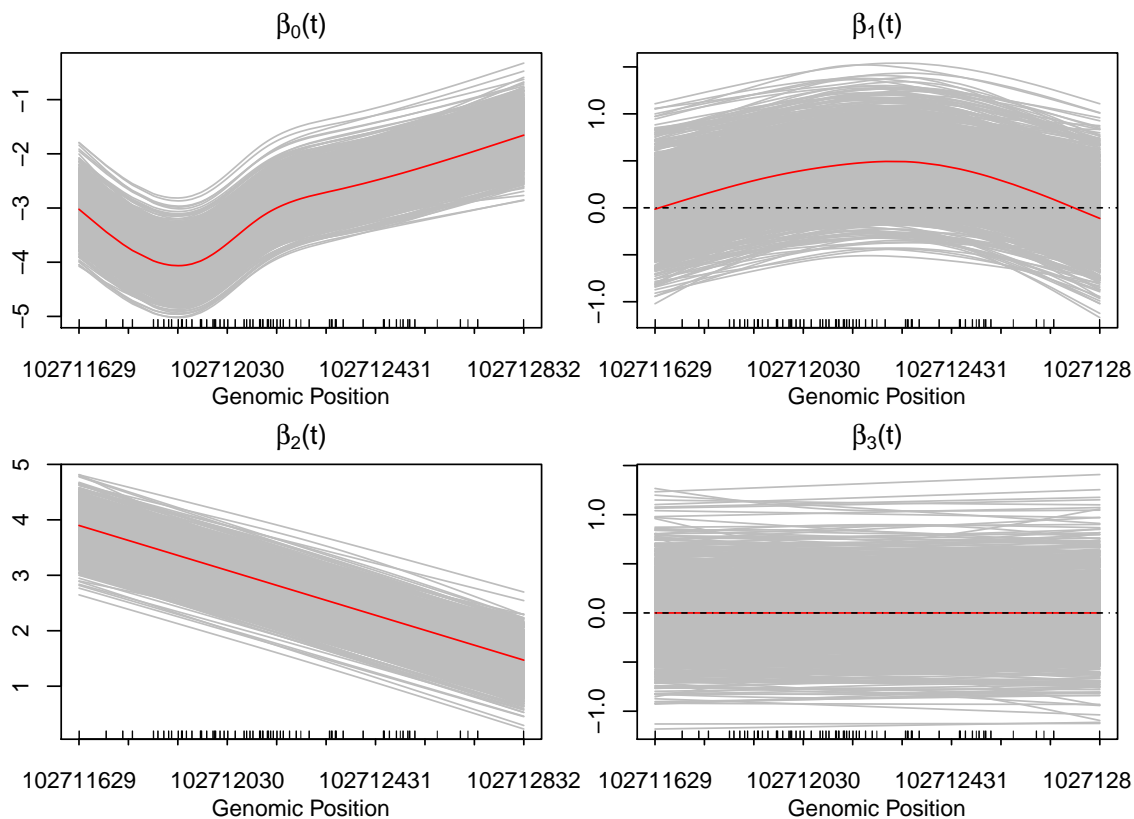


Figure 7. Estimates of smooth covariate effects (gray) over the 1000 simulations in Scenario 1, using dSOMNiBUS. The red curves are the true functional parameters used to generate the data. Data were generated with error using $\phi = 3$ and $\sigma_0^2 = 3$.

with errors.

Figure 8 and 9 demonstrate the performance of the proposed pointwise confidence interval (CI) estimates (Section 4.4.2) and regional test (Section 4.4.3), respectively. The results from dSOMNiBUS are compared to the multiplicative-dispersion-only model and the additive-dispersion-only model. Figure 8 displays the empirical coverage probabilities of the analytical 95% CIs for $\beta_3(t)$, under different settings of ϕ and σ_0^2 . Figure 9 shows the QQ plots for the regional p-values when the null hypothesis $H_0 : \beta_3(t) = 0$ is correct. The results show that ignoring the presence of additive dispersion (i.e. the multiplicative-dispersion-only model) leads to substantial estimation bias, poor CI coverage probabilities and highly inflated type I errors. Although the additive-dispersion-only model provides relatively accurate pointwise CIs, the distributions of its regional p-values are biased away from what would be expected under the null, when multiplicative dispersion $\phi > 1$. Overall, dSOMNiBUS provides point-

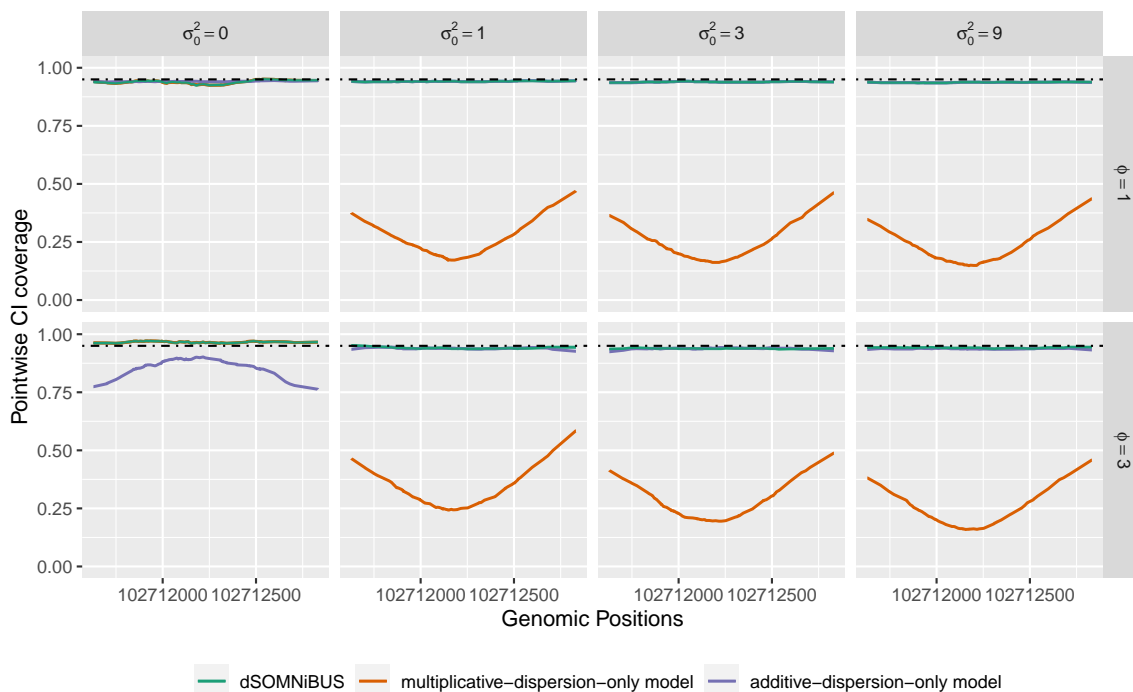


Figure 8. Empirical coverage probability of the analytical 95% CIs for $\beta_3(t)$ over 1000 simulations, under different values of ϕ and σ_0^2 . The empirical coverage probabilities are defined as the percentage of simulations where the analytical CIs cover the true value of $\beta_3(t)$. Data were generated with error, under simulation Scenario 1. The results from dSOMNiBUS (green) and the additive-dispersion-only model (purple) are indistinguishable in all settings but $\sigma_0^2 = 0$ and $\phi = 3$ and dSOMNiBUS (green) and the multiplicative-dispersion-only model (orange) are indistinguishable when $\sigma_0^2 = 0$.

wise CIs attaining their nominal levels, and region-based statistics whose distribution under the null is well calibrated, regardless of the types and degrees of dispersion that data exhibit. Similar results were observed when data were generated without error (Supplementary Figures S5 and S6).

2.3.3 dSOMNiBUS exhibits greater power to detect DMRs while correctly controlling type I error rates

Figures 10 and 11 further demonstrate the performance of the proposed regional test, when compared with the existing methods GlobalTest, dmrseq, BSmooth, SMSC, and BiSeq. Here, data were simulated with error parameters $p_0 = 0.003$ and $1 - p_1 = 0.1$. Figure 10 shows the distributions of p-values for the regional effect of the null covariate

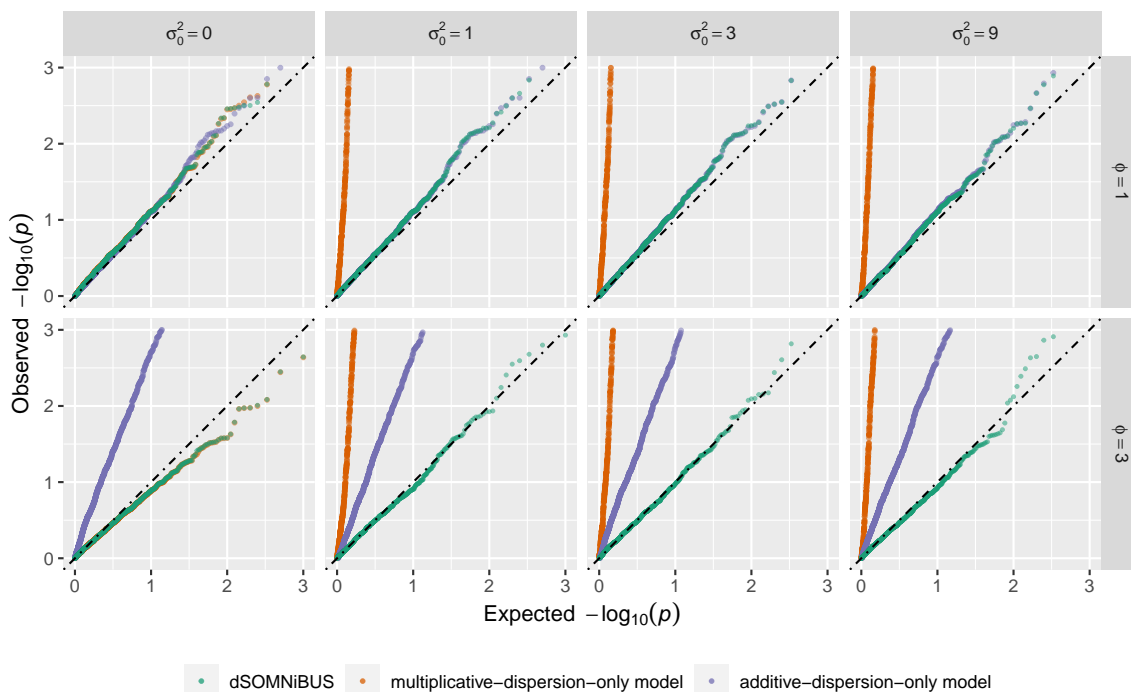


Figure 9. QQ plot for regional p-values for the test $H_0 : \beta_3(t) = 0$, obtained from dSOMNiBUS, the multiplicative-dispersion-only model and the additive-dispersion-only model. Data were simulated with error, under simulation Scenario 1. When $\phi = 1$, the results from dSOMNiBUS (green) and the additive-dispersion-only model (purple) are indistinguishable. When $\sigma_0^2 = 0$, the lines for the multiplicative-dispersion-only model (orange) and dSOMNiBUS (green) are indistinguishable.

Z_3 . Because we estimated the empirical regional p-values for `BSmooth` and `SMSC` by permutations, both methods are able to control type I errors, under all settings of ϕ and σ_0^2 . Both `BiSeq` and `dmrseq` show deflated type I error rate when $\sigma_0^2 = 0$ and inflated type I error rate when $\sigma_0^2 > 0$. The distributions of p-values from `GlobalTest` are well calibrated when the within subject correlation $\sigma_0^2 > 0$, but are slightly biased away from the uniform distribution when $\sigma_0^2 = 0$. When $\sigma_0^2 = 0$ and $\phi = 3$, dSOMNiBUS provides slightly conservative type I errors; this bias vanishes when the data were generated without error (Supplementary Figures S7). Figure 11 shows the powers of the six methods for detecting DMRs under the 15 settings of methylation patterns displayed in Figure 6. Here, methylation difference is defined as the maximum difference between $\pi_1(t)$ and $\pi_0(t)$ in the region. When data exhibit neither additive nor multiplicative dispersion, dSOMNiBUS and `BSmooth` provide the

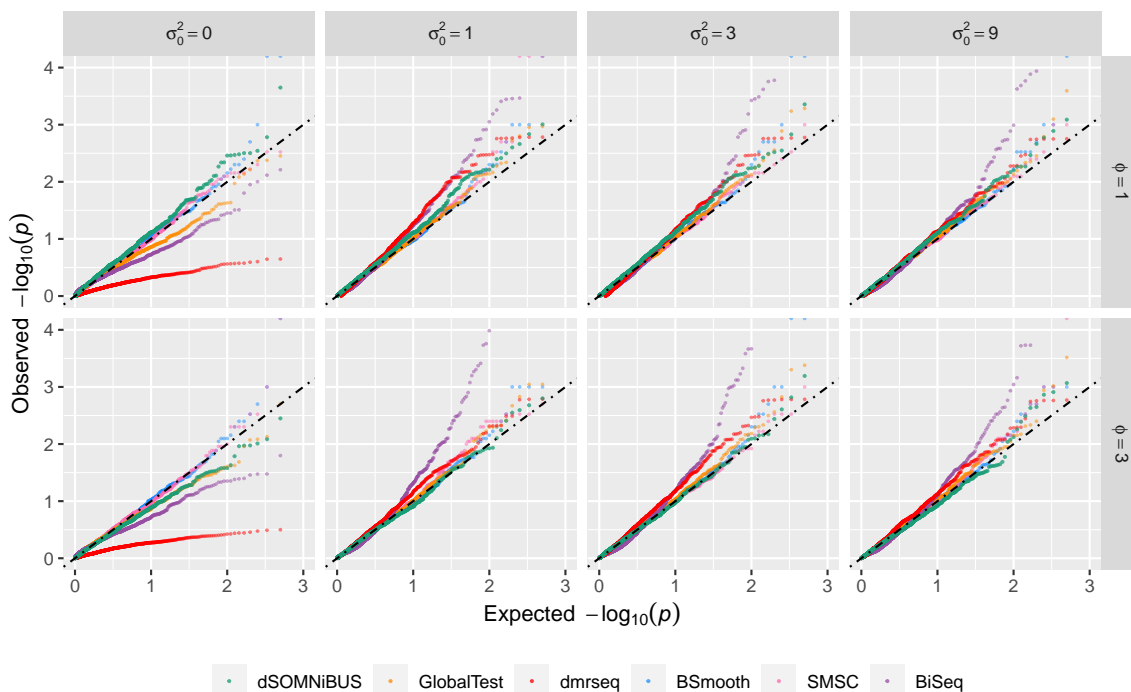


Figure 10. QQ plot for regional p-values for the test $H_0 : \beta_3(t) = 0$, obtained from dSOMNiBUS, GlobalTest, dmrseq, BSmooth, SMSC, and BiSeq. Data were simulated with error, under simulation Scenario 1.

highest power, followed by dmrseq, BiSeq, GlobalTest, and SMSC. When $\sigma_0^2 = 0$ and $\phi = 3$, BSmooth and dmrseq are more powerful than other methods. When there are correlations among methylation measurements on the same subject, i.e. $\sigma_0^2 > 0$, dSOMNiBUS clearly outperforms the five alternative methods; this superiority remains when the data were generated without error (Supplementary Figures S8). In summary, dSOMNiBUS exhibits greater power to detect DMRs, while correctly controlling type I error rates, especially when the regional methylation counts exhibit (additive) extra-binomial variation.

3 Discussion

We have proposed and evaluated a novel method, called dSOMNiBUS, for estimating smooth covariate effects for BS-seq data. We demonstrate that our model, which incorporates both multiplicative and additive sources of data dispersion, provides a plausible representation of realistic dispersion trends in regional methylation data. In

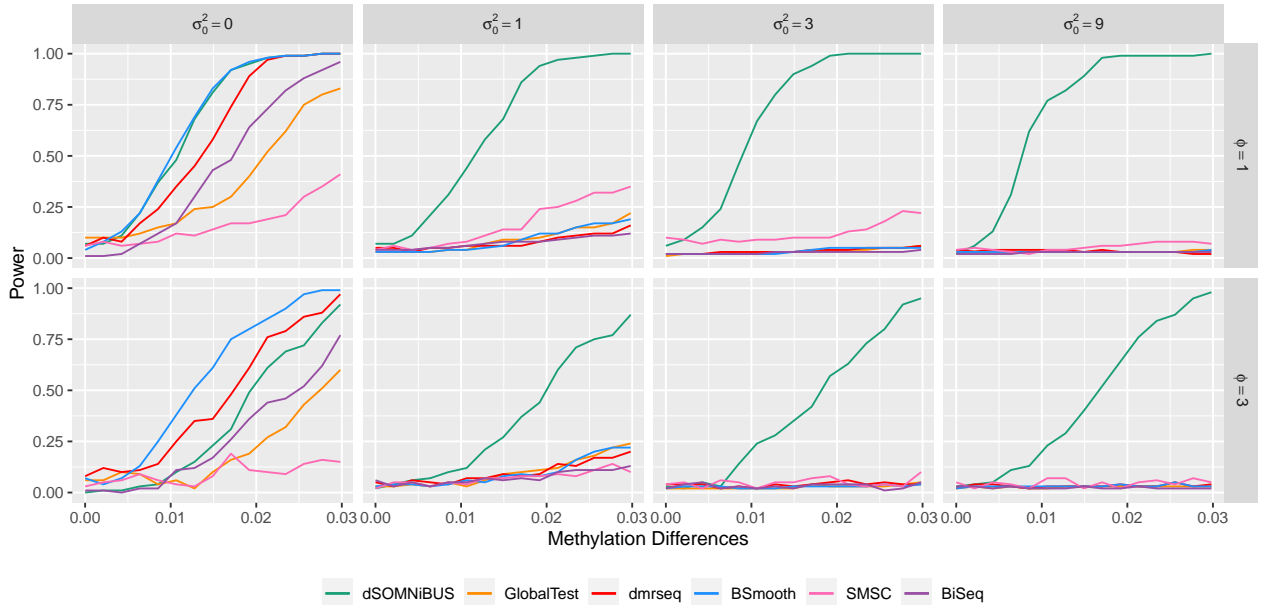


Figure 11. Powers to detect DMRs using the six methods for the 15 simulation settings in Scenario 2 under different levels of maximum methylation differences between $\pi_0(t)$ and $\pi_1(t)$ in the region, calculated over 100 simulations.

addition, dSOMNiBUS simultaneously accounts for experimental errors, estimation of multiple covariate effects, and flexible dispersion patterns in a region. Also, we provide a formal inference for smooth covariate effects and construct a region-based statistic for the test of DMRs, where outcomes might be contaminated by errors and/or exhibit extra-parametric variations. Results from simulations and real data applications show that the new method captures important underlying methylation patterns with excellent power, provides accurate estimates of covariate effects, and correctly quantifies the underlying uncertainty in the estimates. The method has been implemented in the R package `SOMNiBUS`, which has been submitted to R Bioconductor.

Our model captures dispersion in the regional count data via the combination of a subject-specific RE and a multiplicative dispersion. The latter aims to capture the extra random dispersion beyond that introduced by the subject-to-subject variation. An alternative way to add multiplicative dispersion might be to add locus-specific REs. Such model would avoid the problem of estimating ϕ , but would result in substantially increased number of REs, in which case our Laplace approximation is unlikely to provide well-founded inference (Shun and McCullagh, 1995). In addition,

such a model only captures overdispersion. In contrast, our quasi-binomial mixed effect model provides an adequate representation of any kind of dispersion without much increase in computational complexity.

An extension worth exploring in the future is to model the dispersion parameter ϕ as a function of covariates. For example, the methylation variation across cancer samples has been found to be higher than for normal samples (Hansen et al., 2011; Schoofs et al., 2013). Identification of such disease-associated methylation variation changes might provide further insights into the biological mechanisms. This extension would also allow modelling of the hypothesis that some individuals are more sensitive to their environment (Meaney and Szyf, 2005).

Our proposed methods can also be applied to other types of next-generation sequencing data. For example, allele-specific gene expression (ASE) measured from RNA-seq data are quantified by the numbers of reads originating from the two alleles for that site (Fan et al., 2020). Such data share a similar structure to bisulfite sequencing data and could be analyzed by dSOMNiBUS. From the methodology point of view, our proposal of combining quasi likelihood with random effects can be generally applied to any type of count data for a more comprehensive representation of dispersion.

4 Methods and Materials

In this section, we present the methodology details on how to make inference about covariate effects $\beta_p(t_{ij})$ and simultaneously estimate the additive and multiplicative dispersion parameters ϕ and σ_0^2 in our smoothed quasi-binomial mixed model (1). We start with the case where true methylation counts S_{ij} are available, and determine the complete data marginal quasi-likelihood function in Section 4.1. Then we describe the estimating algorithms for the complete and contaminated data in Sections 4.2 and 4.3, respectively. We additionally estimate the pointwise CIs for covariate effects $\beta_p(t_{ij})$ and obtain tests of hypotheses for these effects in Section 4.4.

4.1 Laplace-approximated marginal quasi-likelihood function

4.1.1 Basis representation

In model (1), the function parameters $\beta_p(t_{ij})$ can be represented by the coefficients of chosen spline bases of rank L_p , $\beta_p(t_{ij}) = \sum_{l=1}^{L_p} \alpha_{pl} B_l^{(p)}(t_{ij})$, for $p = 0, 1, \dots, P$. Here $\left\{ B_l^{(p)}(\cdot) \right\}_{l=1}^{L_p}$ denotes the spline basis, and $\boldsymbol{\alpha}_p = (\alpha_{p1}, \dots, \alpha_{pL_p})^T \in \mathcal{R}^{L_p}$ are the coefficients to be estimated. In this way, we can write the conditional mean in (1) in a compact way as

$$g^{-1}(\boldsymbol{\pi}) = \mathbb{X}^{(B)} \boldsymbol{\alpha} + \mathbb{X}^{(1)} \boldsymbol{u},$$

where $\boldsymbol{\pi} = (\pi_{11}, \dots, \pi_{1m_1}, \pi_{21}, \dots, \pi_{2m_2}, \dots, \pi_{Nm_N})^T \in [0, 1]^M$ with $M = \sum_{i=1}^N m_i$, $\boldsymbol{\alpha} = (\boldsymbol{\alpha}_0, \boldsymbol{\alpha}_1, \dots, \boldsymbol{\alpha}_P)^T \in \mathcal{R}^K$ with $K = \sum_{p=0}^P L_p$, and $\boldsymbol{u} = (u_1, u_2, \dots, u_N)^T$. $\mathbb{X}^{(B)}$ is the spanned design matrix for $\boldsymbol{\alpha}$ of dimension $M \times K$, stacked with elements $B_l^{(p)}(t_{ij}) \times Z_{pi}$ with $Z_{0i} \equiv 0$. $\mathbb{X}^{(1)}$ is a random effect model matrix of dimension $M \times N$, with element 1 if the corresponding CpG site in the row belongs to the sample in the column, and 0 otherwise. If we write the overall spanned design matrix $\mathbb{X} = [\mathbb{X}^{(B)}, \mathbb{X}^{(1)}] \in \mathcal{R}^{M \times (K+N)}$ and $\boldsymbol{\mathcal{B}} = (\boldsymbol{\alpha}^T, \boldsymbol{u}^T)^T$, the conditional mean can be further simplified as

$$g^{-1}(\boldsymbol{\pi}) = \mathbb{X} \boldsymbol{\mathcal{B}}.$$

4.1.2 Smoothness penalty

To impose the assumption that the true covariate effect function is more likely to be smooth than jumpy, we add a smoothness penalty for each $\beta_p(t)$, $p = 0, 1, \dots, P$. The total amount of such penalty is an aggregate from all smooth terms, i.e.

$$\mathcal{L}^{\text{Smooth}} = \sum_{p=0}^P \lambda_p \int (\beta_p''(t))^2 dt = \sum_{p=0}^P \lambda_p \boldsymbol{\alpha}_p^T \mathbf{A}_p \boldsymbol{\alpha}_p = \boldsymbol{\alpha}^T \mathbf{A}_\lambda \boldsymbol{\alpha}, \quad (6)$$

where \mathbf{A}_p 's are $L_p \times L_p$ positive semidefinite matrices with the (l, l') element $\mathbf{A}_p(l, l') = \int B_l^{(p)''}(t) B_{l'}^{(p)''}(t) dt$, which are fixed quantities given the specified set of bases. The weights λ_p , i.e. the smoothing parameters, are positive parameters which establish a tradeoff between the closeness of the curve to the data and the smoothness of the fitted curves. \mathbf{A}_λ is a $K \times K$ positive semidefinite block diagonal matrix of the form $\mathbf{A}_\lambda = \text{Diag} \{ \lambda_0 \mathbf{A}_0, \lambda_1 \mathbf{A}_1, \dots, \lambda_P \mathbf{A}_P \}$.

Random-effect view of the smoothness penalty. As justified in Wahba (1983) and Silverman (1985), employing such smoothing penalty (6) during fitting is equivalent to imposing random effects for spline coefficients $\boldsymbol{\alpha}$. Specifically, $\boldsymbol{\alpha}$ is assumed to follow a (degenerate) multivariate normal distribution with precision matrix \mathbf{A}_λ ,

$$\boldsymbol{\alpha} \sim MVN(\mathbf{0}, \mathbf{A}_\lambda^{-}),$$

where \mathbf{A}_λ^{-} is the pseudoinverse of \mathbf{A}_λ . From a Bayesian viewpoint, imposing smoothness is equivalent to specifying a prior distribution on function roughness. This random-effect formulation of the smooth curve estimation problem opens up the possibility of estimating $\boldsymbol{\lambda}$ and ϕ using marginal (quasi-)likelihood maximization. In addition, under such a formulation, it requires no extra effort to estimate the ‘actual’ RE term \mathbf{u} in our model (1), once the inference procedure for $\boldsymbol{\alpha}$ is well established. In the rest of inference steps, we treat $\boldsymbol{\alpha}$ as random effects.

4.1.3 Conditional quasi-likelihood function

We first consider specifying the conditional “distribution” of \mathbf{S} given the values of REs \mathcal{B} . Following the notion of extended quasi-likelihood (McCullagh and Nelder, 1989, Section 9.6), we define the following conditional quasi-likelihood

$$qL^{(\mathbf{S}|\mathcal{B})}(\mathcal{B}, \phi) \propto \exp \left\{ -\frac{1}{2\phi} \sum_{i,j} d_{ij}(S_{ij}, \pi_{ij}) - \frac{M}{2} \log \phi \right\}, \quad (7)$$

where

$$d_{ij}(S_{ij}, \pi_{ij}) = -2 \int_{S_{ij}/X_{ij}}^{\pi_{ij}} \frac{S_{ij} - X_{ij}\pi_{ij}}{\pi_{ij}(1 - \pi_{ij})} d\pi_{ij}$$

is the quasi-deviance function corresponding to a single observation. It can be easily checked that this quasi-likelihood exhibits the properties of log-likelihood, with respect to \mathcal{B} . Such properties approximately hold for the dispersion parameter ϕ , provided that ϕ be small and $\kappa_r = O(\phi^{r-1})$, where κ_r is the r th-order cumulant of $\mathbf{S} | \mathcal{B}$ (Efron, 1986; Jørgensen, 1987; McCullagh and Nelder, 1989). Let $ql^{(\mathbf{S}|\mathcal{B})}(\mathcal{B}, \phi) = \log [qL^{(\mathbf{S}|\mathcal{B})}(\mathcal{B}, \phi)]$ denote the conditional log-quasi-likelihood. It should be noted that the integral inside $qL^{(\mathbf{S}|\mathcal{B})}(\mathcal{B}, \phi)$ rarely needs to be evaluated for the estimation of \mathcal{B} , because the inference described later only requires the computation of its first and second derivatives, i.e.

$$\frac{\partial ql^{(\mathbf{S}|\mathcal{B})}(\mathcal{B}, \phi)}{\partial \mathcal{B}} = \frac{1}{\phi} \mathbb{X}^T (\mathbf{S} - \boldsymbol{\Lambda}_X \boldsymbol{\pi}),$$

$$\frac{\partial^2 q\ell^{(\mathbf{S}|\mathbf{B})}(\mathbf{B}, \phi)}{\partial \mathbf{B} \partial \mathbf{B}^T} = -\frac{1}{\phi} \mathbb{X}^T \mathbf{W} \mathbb{X},$$

where $\mathbf{\Lambda}_X \in \mathbb{R}^{M \times M}$ is the diagonal matrix with values of read-depths, and \mathbf{W} is the weight matrix whose diagonal is $X_{ij}\pi_{ij}(1 - \pi_{ij})$.

4.1.4 Joint quasi-likelihood functions

For notational simplicity, we write $\Theta = (\boldsymbol{\lambda}, \sigma_0^2)$ for the parameters involved in the covariance structure of random effects \mathbf{B} . Combining the conditional ‘distribution’ $\mathbf{S} | \mathbf{B}$ with the marginal distribution of \mathbf{B} , we obtain the following *joint* log-quasi-likelihood of the observed data \mathbf{S} and unobserved random effects \mathbf{B}

$$\begin{aligned} q\ell^{(\mathbf{S}, \mathbf{B})}(\mathbf{B}, \phi, \Theta) &= q\ell^{(\mathbf{S}|\mathbf{B})}(\mathbf{B}, \phi) - \underbrace{\frac{1}{2} \boldsymbol{\alpha}^T \mathbf{A}_\lambda \boldsymbol{\alpha} - \frac{1}{2\sigma_0^2} \mathbf{u}^T \mathbf{u}}_{-\frac{1}{2\phi} \mathbf{B}^T \boldsymbol{\Sigma}_\Theta \mathbf{B}} \\ &\quad + \underbrace{\frac{1}{2} \log \{|\mathbf{A}_\lambda|_+\} + \frac{N}{2} \log (1/\sigma_0^2)}_{1/2 \log \{|\boldsymbol{\Sigma}_\Theta / \phi|_+\}}, \end{aligned} \quad (8)$$

where $\boldsymbol{\Sigma}_\Theta = \text{diag} \{ \phi \mathbf{A}_\lambda, \phi / \sigma_0^2 \mathbf{I}_N \} \in \mathbb{R}^{(K+N) \times (K+N)}$, and $|\bullet|_+$ denotes the generalized determinant of a matrix, i.e. the product of its non-zero eigenvalues. Here we introduce the scaling by ϕ in $\boldsymbol{\Sigma}_\Theta$ merely for later convenience, and this allows us to factor out the dispersion parameter ϕ in the penalized quasi-score in (12). In such way, the point estimates of random effects \mathbf{B} are independent of the estimate of ϕ .

This joint log-quasi-likelihood is composed of three parts: 1) the outcome ‘distribution’ depending on \mathbf{B} and ϕ , 2) multiple quadratic penalties for \mathbf{B} depending on regularization parameters Θ , and 3) fixed regularized terms for Θ . Our goals are to estimate the variance component parameters Θ , the dispersion parameter ϕ , and also predict the values of random effects \mathbf{B} . When $\phi = 1$, this fits a generalized linear mixed model (GLMM).

4.1.5 Laplace-approximated marginal quasi-likelihood function

A legitimate (quasi-)likelihood is the *marginal* ‘density’ evaluated at the observed data \mathbf{S} only, which is obtained by integrating out random effects \mathbf{B} from the joint quasi-likelihood of \mathbf{S} and \mathbf{B} ,

$$qL^M(\phi, \Theta) = \int \exp \{ q\ell^{(\mathbf{S}, \mathbf{B})}(\mathbf{B}, \phi, \Theta) \} d\mathbf{B}. \quad (9)$$

Conceptually, maximizing $qL^M(\phi, \Theta)$ yields the maximum quasi-likelihood estimators for Θ , and ϕ . However, the analytical solutions for this high-dimensional integral are not easy to find, and an approximation approach is needed.

As in Wood (2011), we use the Laplace approximation to evaluate the integral inside the marginal quasi-likelihood. Let $\widehat{\mathbf{B}}_\Theta$ be the value of \mathbf{B} maximizing the joint quasi-likelihood $q\ell^{(\mathbf{S}, \mathbf{B})}(\mathbf{B}, \phi, \Theta)$ given the values of variance component parameters Θ , i.e.

$$\widehat{\mathbf{B}}_\Theta = \operatorname{argmax} \left\{ q\ell^{(\mathbf{S}, \mathbf{B})}(\mathbf{B}, \phi) - \frac{1}{2\phi} \mathbf{B}^T \Sigma_\Theta \mathbf{B} \right\}, \quad (10)$$

where terms not dependent on \mathbf{B} have been dropped from the joint quasi-likelihood. The objective function in (10) is often referred to as the penalized (quasi-)likelihood. A second-order Taylor expansion of $q\ell^{(\mathbf{S}, \mathbf{B})}(\mathbf{B}, \phi, \Theta)$, around $\widehat{\mathbf{B}}$ (the subscript Θ has been dropped for notational simplicity), gives

$$q\ell^{(\mathbf{S}, \mathbf{B})}(\mathbf{B}, \phi, \Theta) \approx q\ell^{(\mathbf{S}, \mathbf{B})}(\widehat{\mathbf{B}}, \phi, \Theta) - \frac{1}{2} (\mathbf{B} - \widehat{\mathbf{B}})^T \mathbf{H}_{\widehat{\mathbf{B}}} (\mathbf{B} - \widehat{\mathbf{B}}),$$

where $\mathbf{H}_{\widehat{\mathbf{B}}} = -\nabla_{\mathbf{B}}^2 q\ell^{(\mathbf{S}, \mathbf{B})}(\widehat{\mathbf{B}}, \phi, \Theta) = \frac{1}{\phi} (\mathbb{X}^T \widehat{\mathbf{W}} \mathbb{X} + \Sigma_\Theta)$. Therefore, the *marginal* quasi-likelihood in (9) can be approximately written as

$$\begin{aligned} qL^M(\phi, \Theta) &\approx \exp \left\{ q\ell^{(\mathbf{S}, \mathbf{B})}(\widehat{\mathbf{B}}, \phi, \Theta) \right\} \int \exp \left\{ -\frac{1}{2} (\mathbf{B} - \widehat{\mathbf{B}})^T \mathbf{H}_{\widehat{\mathbf{B}}} (\mathbf{B} - \widehat{\mathbf{B}}) \right\} d\mathbf{B} \\ &\approx \exp \left\{ q\ell^{(\mathbf{S}, \mathbf{B})}(\widehat{\mathbf{B}}, \phi, \Theta) \right\} \frac{\sqrt{2\pi}^{K+N}}{\left| \frac{\mathbb{X}^T \widehat{\mathbf{W}} \mathbb{X} + \Sigma_\Theta}{\phi} \right|^{1/2}} \\ &\propto \phi^{-M/2} \exp \left(-\frac{\sum_{i,j} \widehat{d}_{ij}}{2\phi} \right) \exp \left(-\frac{1}{2\phi} \widehat{\mathbf{B}}^T \Sigma_\Theta \widehat{\mathbf{B}} \right) |\Sigma_\Theta / \phi|_+^{1/2} \left| \frac{\mathbb{X}^T \widehat{\mathbf{W}} \mathbb{X} + \Sigma_\Theta}{\phi} \right|^{-1/2}. \end{aligned} \quad (11)$$

In equation (11), $\widehat{d}_{ij} = d_{ij}(S_{ij}, \widehat{\pi}_{ij})$, where $\widehat{\pi}_{ij} = g^{-1}(\mathbb{X}_{(i), \widehat{\mathbf{B}}})$ and l is the row in the model matrix \mathbb{X} corresponding to CpG j for sample i . We denote this Laplace-approximated marginal quasi-likelihood in (11) as $qL^{\text{Laplace}}(\phi, \Theta; \widehat{\mathbf{B}})$ and simply write $\text{Laplace}(\phi, \Theta; \widehat{\mathbf{B}}) = \log[qL^{\text{Laplace}}(\phi, \Theta; \widehat{\mathbf{B}})]$, which depends on Θ via the dependence of Σ_Θ and $\widehat{\mathbf{B}}$ (and thus $\widehat{\mathbf{W}}$ and $\widehat{\mathbf{d}}$) on Θ .

4.2 Estimation algorithm for the complete data

The essence of estimating Θ, \mathcal{B} , and ϕ , is to optimize the Laplace-approximated marginal quasi-likelihood in (11). Note that such approximation requires calculating the maximum of the penalized quasi-likelihood in (10), $\widehat{\mathcal{B}}$, along with its corresponding Hessian $\mathbf{H}_{\widehat{\mathcal{B}}}$, which is only feasible for given values of the penalty parameters Θ . To disentangle the complicated dependence of $\widehat{\mathcal{B}}$ on Θ , we adopt a nested-optimization strategy proposed by Wood (2011). Specifically, the algorithm has an outer iteration for updating Θ and ϕ , with each iterative step supplementing with an inner iteration to estimate random effects \mathcal{B} corresponding to the current Θ , as summarized in Algorithm 1. This Section proceeds with the detailed description of each step in Algorithm 1.

Algorithm 1: Algorithm to find $(\widehat{\mathcal{B}}, \widehat{\phi}, \widehat{\Theta}) = \operatorname{argmax}_{\mathcal{B}, \phi, \Theta} \ell^{(\mathcal{S}, \mathcal{B})}(\mathcal{B}, \phi, \Theta)$ using data $\{\mathcal{S}, \mathbf{Z}, \mathbf{Y}\}$

Initialize $\Theta^{(0)}, \phi^{(0)}$; Choose $\varepsilon = 10^{-6}$; Set $s = 0$;

repeat

Step 1. Solve $\mathbf{U}(\mathcal{B}; \Theta^{(s)}) = \mathbf{0}$ (12) to obtain $\mathcal{B}^{(s)}$;

Step 2. Newton's update for the Laplace-approximated marginal likelihood

$$(\log(\phi), \log(\Theta))^{(s+1)} = (\log(\phi), \log(\Theta))^{(s)} - \left[\nabla^2 \text{Laplace}(\mathcal{B}^{(s)}) \right]^{-1} \nabla \text{Laplace}(\mathcal{B}^{(s)});$$

$s \leftarrow s + 1$;

until $\|\mathcal{B}^{(s)} - \mathcal{B}^{(s-1)}\|_2 < \varepsilon$;

Return $\Theta^{(s)}, \mathcal{B}^{(s)}, \phi^{(s)}$;

Step 3: Calculate $\widehat{\phi}_{Flc}$ using $\mathcal{B}^{(s)}$

4.2.1 Inner iteration: estimate \mathcal{B} given the current Θ

Given the estimates of penalty parameters Θ , $\widehat{\mathcal{B}}$ can be computed as the solution to

$$\mathbf{U}(\mathcal{B}) = \frac{1}{\phi} \{ \mathbb{X}^T (\mathcal{S} - \Lambda_{\mathbf{X}} \boldsymbol{\pi}) - \Sigma_{\Theta} \mathcal{B} \} = \mathbf{0}, \quad (12)$$

where $\mathbf{U}(\mathcal{B})$ is the *quasi-score* for the penalized quasi-likelihood in (10) with respect to \mathcal{B} . We use the Newton's method to solve these system of nonlinear equations.

Specifically we compute the gradient of $U(\mathbf{B})$,

$$\nabla U(\mathbf{B}) = -\frac{\mathbb{X}^T \mathbf{W} \mathbb{X} + \Sigma_{\Theta}}{\phi},$$

and a single update from step l to step $l + 1$ for \mathbf{B} thus takes the form

$$\mathbf{B}^{(l+1)} = \mathbf{B}^{(l)} + (\mathbb{X}^T \mathbf{W} \mathbb{X} + \Sigma_{\Theta})^{-1} \left[\mathbb{X}^T (\mathbf{S} - \Lambda_{\mathbf{X}} \boldsymbol{\pi}^{(l)}) - \Sigma_{\Theta} \mathbf{B}^{(l)} \right].$$

We then iteratively update \mathbf{B} until convergence, which constitutes iteration Step 1 in Algorithm 1.

4.2.2 Outer iteration: maximize the Laplace-approximated marginal quasi-likelihood

The outer iteration, which aims to maximize the Laplace-approximated marginal quasi-likelihood in (11), is also achieved by a Newton's method. Wood (2011) has derived the derivatives and Hessian of $\text{Laplace}(\phi, \Theta; \hat{\mathbf{B}})$ with respect to $\boldsymbol{\rho} = (\log(\Theta), \log(\phi))$, using a mixture of implicit and direct differentiations. We denote these first and second derivatives as $\nabla \text{Laplace}(\boldsymbol{\rho}; \hat{\mathbf{B}})$ and $\nabla^2 \text{Laplace}(\boldsymbol{\rho}; \hat{\mathbf{B}})$, respectively. Relying on the work of Wood (2011), the maximization in the outer iteration can be readily achieved via

$$\boldsymbol{\rho}^{(s+1)} = \boldsymbol{\rho}^{(s)} - \left[\nabla^2 \text{Laplace}(\boldsymbol{\rho}^{(s)}; \hat{\mathbf{B}}^{(s)}) \right]^{-1} \nabla \text{Laplace}(\boldsymbol{\rho}^{(s)}; \hat{\mathbf{B}}^{(s)}). \quad (13)$$

Here, $\hat{\mathbf{B}}^{(s)}$ are the estimated mean parameters given the current $\Theta^{(s)}$, obtained from the inner iteration in Section 4.2.1. Each update in (13) constitutes iteration Step 2 in Algorithm 1. We iterate between the Step 1 and Step 2 until convergence to obtain $\hat{\mathbf{B}}, \hat{\Theta}$ and $\hat{\phi}$.

4.2.3 Estimating ϕ using the moment-based estimator

As described in the previous section, the dispersion parameter ϕ can be estimated as part of the outer iteration of the marginal quasi-likelihood maximization. We refer to this estimator as likelihood-based dispersion estimator, denoted as $\hat{\phi}_{Lik}$.

In generalized linear models, it is common to estimate ϕ by dividing Pearson's lack-of-fit statistic by the residual degrees of freedom, and this is known as the moment-based scale/dispersion estimator. We can apply the similar ideas here. Instead of

using $\widehat{\phi}_{Lik}$, we take one step further and estimate ϕ using the final estimate $\widehat{\mathbf{B}}$ (and thus $\widehat{\boldsymbol{\pi}}$). Specifically, Pearson’s dispersion estimator can be written as

$$\widehat{\phi}_P = \frac{1}{M - \tau} \sum_{i,j} \left(\frac{S_{ij} - X_{ij}\widehat{\pi}_{ij}}{\sqrt{X_{ij}\widehat{\pi}_{ij}(1 - \widehat{\pi}_{ij})}} \right)^2.$$

Here τ is the effective degrees of freedom (Wood, 2017), defined as

$$\tau = \text{trace}(\mathbf{F}), \text{ with } \mathbf{F} = \left(\mathbb{X}^T \widehat{\mathbf{W}} \mathbb{X} + \boldsymbol{\Sigma}_{\widehat{\boldsymbol{\theta}}} \right)^{-1} \mathbb{X}^T \widehat{\mathbf{W}} \mathbb{X}. \quad (14)$$

However, $\widehat{\phi}_P$ can be unstable at finite sample sizes, especially when a few Pearson residuals are huge (Farrington, 1995; Fletcher, 2012). For example, in our model, $\widehat{\pi}_{ij}$ close to 0 can lead to a huge Pearson residual, even though the deviance $d_{ij}(S_{ij}, \widehat{\pi}_{ij})$ in (7) is modest. Therefore, we adopt an improved version of the Pearson estimator, i.e. the Fletcher estimator (Fletcher, 2012), which is designed to mitigate this problem. The Fletcher’s dispersion estimator $\widehat{\phi}_{Fle}$ is defined as

$$\widehat{\phi}_{Fle} = \frac{\widehat{\phi}_P}{1 + \bar{a}}, \text{ where } a_{ij} = \frac{1 - 2\widehat{\pi}_{ij}}{X_{ij}\widehat{\pi}_{ij}(1 - \widehat{\pi}_{ij})} (S_{ij} - X_{ij}\widehat{\pi}_{ij}) \text{ and } \bar{a} = \frac{1}{M} \sum_{i,j} a_{ij}.$$

If the mean model is adequate, then approximately we have

$$\frac{(M - \tau)\widehat{\phi}_{Fle}}{\phi} \sim \chi_{M-\tau}^2 \quad (15)$$

(McCullagh, 1985; Fletcher, 2012). Therefore, $\widehat{\phi}_{Fle}$ provides an unbiased estimator for ϕ , which is also confirmed by simulation results as shown in Supplementary Figure S9. In contrast, the estimation using $\widehat{\phi}_{Lik}$ can be considerably biased (Supplementary Figure S9). Hence, we calculate the moment-based estimate for the dispersion parameter, which constitutes the Step 3 in Algorithm 1.

4.3 Estimating algorithm for the contaminated data

In the presence of experimental errors, the true methylation data, S_{ij} are unknown and one only observes Y_{ij} , which is assumed to be a mixture of binomial counts arising from both the truly methylated and truly unmethylated reads. When S_{ij} is modeled by a parametric distribution, like in Zhao et al. (2020), the EM algorithm (Dempster et al., 1977) provides accurate estimation of the smooth covariate effects even though the true methylation data are missing. Motivated by the work of Elashoff and Ryan (2004), we propose an extension of the EM algorithm with special treatment for the multiplicative dispersion parameter ϕ , to the case of quasi-likelihood-based analyses.

4.3.1 Expectation-Solving algorithm

Elashoff and Ryan (2004) proposed an extension of the EM algorithm, called Expectation-Solving (ES) algorithm, to accommodate missing (or mis-measured) data when a natural set of estimating equations exists for the complete data setting. Specifically, the E step computes the conditional expectation of the estimating equations given the observed data, and S step solves these expected estimating equations.

To apply the ES algorithm to our case, we need to evaluate the conditional expectation of three sets of estimating equations:

$$\begin{aligned} U(\mathbf{B}; \Theta^{(s)}, \mathbf{S}) &= \frac{1}{\phi} [\mathbb{X}^T (\mathbf{S} - \Lambda_{\mathbf{X}} \boldsymbol{\pi}^{(s)}) - \Sigma_{\Theta^{(s)}} \mathbf{B}] = \mathbf{0} \\ \nabla_{\Theta} \text{Laplace}(\Theta, \phi; \mathbf{B}^{(s)}, \mathbf{S}) &= \frac{1}{\phi} \sum_{i,j} \left\{ \frac{S_{ij} - X_{ij} \pi_{ij}^{(s)}}{\pi_{ij}^{(s)} (1 - \pi_{ij}^{(s)})} \times \frac{d\pi_{ij}^{(s)}}{d\Theta} \right\} + f_1(\Theta, \phi; \mathbf{B}^{(s)}) = \mathbf{0} \\ \nabla_{\phi} \text{Laplace}(\Theta, \phi; \mathbf{B}^{(s)}, \mathbf{S}) &= \frac{1}{\phi^2} \sum_{i,j} \int_{S_{ij}/X_{ij}}^{\pi_{ij}^{(s)}} \frac{S_{ij} - X_{ij} \pi_{ij}}{\pi_{ij} (1 - \pi_{ij})} d\pi_{ij} + f_2(\Theta, \phi; \mathbf{B}^{(s)}) = \mathbf{0}, \end{aligned}$$

for \mathbf{B} , Θ and ϕ , respectively. Here, $\Theta^{(s)}$, $\mathbf{B}^{(s)}$, and $\boldsymbol{\pi}^{(s)}$ are estimates from the previous iterations, $f_1(\cdot)$ and $f_2(\cdot)$ denote the components that are independent of \mathbf{S} .

E step for \mathbf{B} and \mathbf{S} . The estimating equations for \mathbf{B} and Θ are linear in the latent methylated counts \mathbf{S} , and thus their expectations equal $U(\mathbf{B}; \Theta^{(s)}, \boldsymbol{\eta}^*)$ and $\nabla_{\Theta} \text{Laplace}(\Theta, \phi; \mathbf{B}^{(s)}, \boldsymbol{\eta}^*)$, respectively. Here, $\boldsymbol{\eta}^* \in \mathcal{R}^M$ are the conditional expectations of \mathbf{S} given \mathbf{Y} evaluated at the trial estimates (\mathbf{B}^*, Θ^*) , and for our model, take the form

$$\eta_{ij}^* = \mathbb{E}(S_{ij} | Y_{ij}; \mathbf{B}^*, \Theta^*) = \frac{Y_{ij} p_1 \pi_{ij}^*}{p_1 \pi_{ij}^* + p_0 (1 - \pi_{ij}^*)} + \frac{(X_{ij} - Y_{ij}) (1 - p_1) \pi_{ij}^*}{(1 - p_1) \pi_{ij}^* + (1 - p_0) (1 - \pi_{ij}^*)}, \quad (16)$$

where $\pi_{ij}^* = g^{-1}(\mathbb{X}_{(l,i)} \mathbf{B}^*)$ and l is the row in the model matrix \mathbb{X} corresponding to CpG j for sample i . These expected estimating equations can then be solved using the direct nested iteration method in Algorithm 1.

E step for ϕ . However, the estimating equation for ϕ is not linear in the unknown methylated counts \mathbf{S} ; see details in Appendix B.1. Therefore, the closed-form exact expression for $\mathbb{E}_{\mathbf{S}|\mathbf{Y}; \mathbf{B}^*, \Theta^*}(\nabla_{\phi} \text{Laplace}(\Theta, \phi; \mathbf{B}^{(s)}, \mathbf{S}))$ is not available, and the E-S algorithm cannot be readily applied to estimating ϕ from the contaminated data. To

circumvent this problem, we propose a direct method to estimate ϕ without undergoing the E-S iteration.

4.3.2 A plug-in estimator for ϕ

Specifically, we estimate ϕ by exploiting its relationship with the dispersion for the observed outcome \mathbf{Y} , denoted as ϕ_{ij}^Y , which is defined as

$$\phi_{ij}^Y = \frac{\text{Var}(Y_{ij} | u_i)}{X_{ij}\pi_{ij}^Y(1 - \pi_{ij}^Y)}, \text{ with } \pi_{ij}^Y = \mathbb{E}(Y_{ij} | u_i) = \pi_{ij}p_1 + (1 - \pi_{ij})p_0.$$

Based on our assumed mean-variance relationship (2) and error model (5), we can express ϕ_{ij}^Y in terms of ϕ , π_{ij} and error parameters p_0 and p_1 ,

$$\phi_{ij}^Y = 1 + (\phi - 1) \frac{(\pi_{ij}^Y - p_0)(p_1 - \pi_{ij}^Y)}{\pi_{ij}^Y(1 - \pi_{ij}^Y)}; \quad (17)$$

see detailed derivations in Appendix B.2. Although we assume a constant dispersion ϕ for the true outcome \mathbf{S} , the observed outcome \mathbf{Y} implied by our error model, possesses dispersion parameter ϕ_{ij}^Y varying with each CpG site, when $\phi \neq 1$.

Directly running the nested iteration method (Algorithm 1) on the observed data $\{\mathbf{Y}, \mathbf{Z}, \mathbf{X}\}$ reports a constant dispersion estimate $\widehat{\phi}^Y$ and $\widehat{\pi}_{ij}^Y$ for all i and j , along with other useful estimates. We assume that $\widehat{\phi}^Y$ is an estimate for the mean of individual dispersions ϕ_{ij}^Y , i.e.

$$\frac{1}{M} \sum_{i,j} \phi_{ij}^Y = 1 + (\phi - 1) \frac{1}{M} \sum_{i,j} \frac{(\pi_{ij}^Y - p_0)(p_1 - \pi_{ij}^Y)}{\pi_{ij}^Y(1 - \pi_{ij}^Y)}; \quad (18)$$

empirical results show that this is a reasonable assumption, as shown in Supplementary Figure S11. We then propose to estimate ϕ by plugging in the error-prone outcome-related estimates $\widehat{\phi}^Y$ and $\widehat{\pi}_{ij}^Y$ to the relation in (18):

$$\widehat{\phi} = (\widehat{\phi}^Y - 1) \left[\frac{1}{M} \sum_{i,j} \frac{(\widehat{\pi}_{ij}^Y - p_0)(p_1 - \widehat{\pi}_{ij}^Y)}{\widehat{\pi}_{ij}^Y(1 - \widehat{\pi}_{ij}^Y)} \right]^{-1} + 1.$$

4.3.3 A hybrid ES algorithm

We propose a hybrid ES algorithm to estimate our model using the error-prone outcomes \mathbf{Y} . We first estimate ϕ using the aforementioned plug-in approach and then estimate \mathbf{B} and Θ using ES iterations assuming ϕ is fixed and known; detailed steps

are summarized in Algorithm 2. We denote the final estimates from our algorithm as $\widehat{\phi}$, $\widehat{\mathbf{B}}$ and $\widehat{\Theta}$. The components of $\widehat{\alpha}$ inside the vector of $\widehat{\mathbf{B}}$ leads to estimates of the functional parameters $\beta_p(t)$, for $p = 0, 1, \dots, P$:

$$\widehat{\beta}_p(t) = \left\{ \mathbf{B}^{(p)}(t) \right\}^T \{ \widehat{\alpha}_p \},$$

where t is a genomic position lying within the range of the input positions $\{t_{ij}\}$, and $\mathbf{B}^{(p)}(t) = (B_1^{(p)}(t), B_2^{(p)}(t), \dots, B_{L_p}^{(p)}(t))^T \in \mathcal{R}^{L_p}$ is a column vector with nonrandom quantities obtained from evaluating the set of basis functions $\{B_l^{(p)}(\cdot)\}_l$ at position t .

Algorithm 2: A hybrid ES algorithm to estimate the smoothed quasi-binomial mixed model with error-prone outcomes.

Step 1: run Algorithm 1 on $\{\mathbf{Y}, \mathbf{Z}, \mathbf{X}\}$; return $\widehat{\pi}^Y$, $\widehat{\phi}_Y$, $\widehat{\mathbf{B}}$, and $\widehat{\Theta}$;

Step 2: calculate the plug-in estimator $\widehat{\phi}$;

Step 3: E-S iterations with ϕ fixed at $\widehat{\phi}$ to estimate \mathbf{B} and Θ ; specifically

Initialize $\Theta^{(0)} = \widehat{\Theta}$, $\mathbf{B}^{(0)} = \widehat{\mathbf{B}}$; Choose $\varepsilon = 10^{-6}$; Set $\ell = 0$;

repeat

• E step: $\eta_{ij}^{(\ell)} = \mathbb{E}(S_{ij} | Y_{ij}; \mathbf{B}^{(\ell)})$;

• S step: $(\mathbf{B}^{(\ell)}, \Theta^{(\ell)}) = \operatorname{argmax}_{\mathbf{B}, \Theta} \ell^{(\mathbf{B}, \Theta)}(\mathbf{B}, \Theta; \eta_{ij}^{(\ell)}, \widehat{\phi})$. Specifically

repeat

• Solve $\mathbf{U}(\mathbf{B}; \Theta^{(s)}; \boldsymbol{\eta}^{(\ell)}) = \mathbf{0}$ to obtain $\mathbf{B}^{(s)}$ using data $\eta_{ij}^{(\ell)}$;

• Newton's update for the Laplace approximated marginal likelihood evaluated at data $\eta_{ij}^{(\ell)}$:

$$(\log \Theta)^{(s+1)} = (\log \Theta)^{(s)} - \left[\nabla_{\Theta}^2 \text{Laplace}(\mathbf{B}^{(s)}) \right]^{-1} \nabla_{\Theta} \text{Laplace}(\mathbf{B}^{(s)});$$

$s \leftarrow s + 1$;

until $\|\mathbf{B}^{(s)} - \mathbf{B}^{(s-1)}\|_2 < \varepsilon$;

$\ell \leftarrow \ell + 1$;

until $\|\mathbf{B}^{(\ell)} - \mathbf{B}^{(\ell-1)}\|_2 < \varepsilon$;

Return $\Theta^{(\ell)}, \mathbf{B}^{(\ell)}$;

4.4 Inference for smooth covariate effects

We then estimate the pointwise confidence intervals (CI) for the smoothed covariate effects $\{\beta_1(t), \beta_2(t), \dots, \beta_P(t)\}$, and obtain tests of hypotheses for these effects. Note

that the inference is carried out conditional on the values of variance component parameters Θ and dispersion parameter ϕ , i.e. the uncertainty in estimating them is not accounted for.

4.4.1 Estimating the variance of the resulting parameter estimates

As did in [Elashoff and Ryan \(2004\)](#), we can re-express the E step as the solution to the following M-dimensional estimating equation:

$$\mathbf{U}^{(2)}(\mathbf{S}) = \mathbf{S} - \hat{\boldsymbol{\eta}} = \mathbf{0},$$

where $\hat{\boldsymbol{\eta}}$ are the conditional expectations in (16) evaluated at the current estimate $\hat{\boldsymbol{\pi}}$. In this way, the overall ES algorithm can be viewed as solving an expanded set of equations of dimension $K + N + M$, whose first $K + N$ components are $\mathbf{U}(\mathbf{B}) = \mathbf{0}$ in (12) and whose second M components are $\mathbf{U}^{(2)}(\mathbf{S}) = \mathbf{0}$.

Under this formulation, we use the established theory for estimating equations ([Lindsay, 1982](#); [Heyde and Morton, 1996](#); [Small et al., 2003](#)), and propose a model-based variance estimator for $\hat{\mathbf{B}}$. Specifically, under correct specification of the first two moments of \mathbf{S} , the asymptotic variance of $\hat{\mathbf{B}}$ can be written as

$$\text{Var}(\hat{\mathbf{B}}) = [(-\mathbf{D})^{-1}]_{(\mathbf{B}, \mathbf{B})},$$

where \mathbf{D} is the first order derivative of the expanded estimating equations for \mathbf{B} and \mathbf{S} , and $[\bullet]_{(\mathbf{B}, \mathbf{B})}$ stands for the matrix block corresponding to \mathbf{B} . In our case, \mathbf{D} takes the form

$$\mathbf{D} = - \begin{bmatrix} \frac{1}{\phi} \mathbb{X}^T \mathbf{W} \mathbb{X} + \frac{1}{\phi} \boldsymbol{\Sigma}_{\Theta} & -\frac{1}{\phi} \mathbb{X}^T \\ \mathbf{W}_{\delta} \mathbb{X} & -\mathbf{I}_M. \end{bmatrix}$$

Here, \mathbf{W}_{δ} is a diagonal matrix with elements $X_{ij}\delta_{ij}$, where

$$\delta_{ij} = \frac{Y_{ij}p_1p_0}{[p_1\pi_{ij} + p_0(1 - \pi_{ij})]^2} + \frac{(X_{ij} - Y_{ij})(1 - p_1)(1 - p_0)}{[(1 - p_1)\pi_{ij} + (1 - p_0)(1 - \pi_{ij})]^2},$$

and reduces to a zero matrix when $p_0 = 1 - p_1 = 0$. Then, the asymptotic variance of $\hat{\mathbf{B}}$ can be simplified as

$$\text{Var}(\hat{\mathbf{B}}) = [\mathbb{X}^T (\mathbf{W} - \mathbf{W}_{\delta}) \mathbb{X} + \boldsymbol{\Sigma}_{\Theta}]^{-1} \phi. \quad (19)$$

Therefore, the desired variance estimator of $\hat{\mathbf{B}}$ can be obtained by plugging in the final estimates $\hat{\mathbf{B}}$, $\hat{\Theta}$ and $\hat{\phi}$ into equation (19).

4.4.2 Confidence interval estimation

Let $\widehat{\mathbf{V}}$ denote the aforementioned variance estimator and $\widehat{\mathbf{V}}_p$ be the diagonal blocks of $\widehat{\mathbf{V}}$ corresponding to $\boldsymbol{\alpha}_p$, with dimensions $L_p \times L_p$. We then immediately have the estimated variance of $\widehat{\beta}_p(t)$: $\widehat{\text{Var}}(\widehat{\beta}_p(t)) = \left\{ \mathbf{B}^{(p)}(t) \right\}^T \widehat{\mathbf{V}}_p \left\{ \mathbf{B}^{(p)}(t) \right\}$. Therefore, the confidence interval for $\widehat{\beta}_p(t)$ at significance level ν can be approximately estimated by $\widehat{\beta}_p(t) \pm \mathbb{Z}_{\nu/2} \sqrt{\widehat{\text{Var}}(\widehat{\beta}_p(t))}$, for any t in the range of interest, where $\mathbb{Z}_{\nu/2}$ is $\nu/2$ (upper-tail) quantile of a standard normal distribution.

4.4.3 Hypothesis testing for a regional zero effect

We can also construct a region-wide test of the null hypothesis

$$H_0 : \beta_p(t) = 0, \text{ for any } t \text{ in the genomic interval.}$$

This test depends on the association between covariate Z_p and methylation levels across the region, after adjustment for all the other covariates, and the null hypothesis is equivalent to $H_0 : \boldsymbol{\alpha}_p = \mathbf{0}$. We propose the following region-based F statistic

$$T_p = \frac{\widehat{\boldsymbol{\alpha}}_p^T \left\{ \widehat{\mathbf{V}}_p \right\}^{-1} \widehat{\boldsymbol{\alpha}}_p}{\tau_p},$$

where $\left\{ \widehat{\mathbf{V}}_p \right\}^{-1}$ denotes inverse if $\widehat{\mathbf{V}}_p$ is nonsingular; for singular $\widehat{\mathbf{V}}_p$, the inverse is replaced by the Moore-Penrose inverse $\left\{ \widehat{\mathbf{V}}_p \right\}^-$. Here, τ_p is the effective degrees of freedom (EDF) for smooth term $\beta_p(t)$, which depends on the magnitude of smoothing parameter $\boldsymbol{\lambda}$ and random effect variances σ_0^2 . Motivated by the work of Wood (2013), we define the EDF τ_p as

$$\tau_p = \sum_{l=a_p}^{b_p} (2\mathbf{F} - \mathbf{F}\mathbf{F})_{(l,l)}, \text{ for } p = 0, 1, \dots, P,$$

where $a_p = \sum_{m=0}^{p-1} L_m + 1$ if $p > 0$ and $a_p = 1$ if $p = 0$, $b_p = \sum_{m=0}^p L_m$ for any p , and $(\bullet)_{(l,l)}$ stands for the l^{th} leading diagonal element of a matrix. \mathbf{F} is the smoothing matrix of our model, as defined in (14), which can be viewed as the matrix mapping the pseudo data to its predicted mean.

Let $\mathbf{V}_p = \widehat{\mathbf{V}}_p \cdot \phi / \widehat{\phi}$ be the variance estimator for $\boldsymbol{\alpha}_p$ when the dispersion parameter ϕ is known. Zhao et al. (2020) have shown the following asymptotic results under the null

$$\widehat{\boldsymbol{\alpha}}_p^T \left\{ \mathbf{V}_p \right\}^{-1} \widehat{\boldsymbol{\alpha}}_p \sim \chi_{\tau_p}^2.$$

Combining with the property of moment-based dispersion estimator in (15), we can conclude that, under the null hypothesis, T_p asymptotically follows a F distribution with degrees of freedom τ_p and $M - \tau$, i.e. $T_p \sim F_{\tau_p, M-\tau}$.

References

- Akalin, A., Kormaksson, M., Li, S., Garrett-Bakelman, F. E., Figueroa, M. E., Melnick, A., and Mason, C. E. (2012). methylkit: a comprehensive r package for the analysis of genome-wide dna methylation profiles. *Genome biology*, 13(10):1–9.
- Allum, F., Hedman, Å. K., Shao, X., Cheung, W. A., Vijay, J., Guénard, F., Kwan, T., Simon, M.-M., Ge, B., Moura, C., et al. (2019). Dissecting features of epigenetic variants underlying cardiometabolic risk using full-resolution epigenome profiling in regulatory elements. *Nature communications*, 10(1):1–13.
- Allum, F., Shao, X., Guénard, F., Simon, M.-M., Busche, S., Caron, M., Lambourne, J., Lessard, J., Tandre, K., Hedman, Å. K., et al. (2015). Characterization of functional methylomes by next-generation capture sequencing identifies novel disease-associated variants. *Nature communications*, 6(1):1–12.
- Breslow, N. E. and Clayton, D. G. (1993). Approximate inference in generalized linear mixed models. *Journal of the American statistical Association*, 88(421):9–25.
- Browne, W. J., Subramanian, S. V., Jones, K., and Goldstein, H. (2005). Variance partitioning in multilevel logistic models that exhibit overdispersion. *Journal of the Royal Statistical Society: Series A (Statistics in Society)*, 168(3):599–613.
- Cheng, L. and Zhu, Y. (2013). A classification approach for dna methylation profiling with bisulfite next-generation sequencing data. *Bioinformatics*, 30(2):172–179.
- Choy, M.-K., Movassagh, M., Goh, H.-G., Bennett, M. R., Down, T. A., and Foo, R. S. (2010). Genome-wide conserved consensus transcription factor binding motifs are hyper-methylated. *BMC genomics*, 11(1):519.
- Cui, S., Ji, T., Li, J., Cheng, J., and Qiu, J. (2016). What if we ignore the random effects when analyzing rna-seq data in a multifactor experiment. *Statistical applications in genetics and molecular biology*, 15(2):87–105.

- Davison, A. C. and Hinkley, D. V. (1997). *Bootstrap methods and their application*. Number 1. Cambridge university press.
- Dempster, A. P., Laird, N. M., and Rubin, D. B. (1977). Maximum likelihood from incomplete data via the em algorithm. *Journal of the Royal Statistical Society. Series B (Statistical Methodology)*, pages 1–38.
- Dolinoy, D. C., Huang, D., and Jirtle, R. L. (2007). Maternal nutrient supplementation counteracts bisphenol a-induced dna hypomethylation in early development. *Proceedings of the National Academy of Sciences*, 104(32):13056–13061.
- Dolzhenko, E. and Smith, A. D. (2014). Using beta-binomial regression for high-precision differential methylation analysis in multifactor whole-genome bisulfite sequencing experiments. *BMC bioinformatics*, 15(1):215.
- Dunaway, K. W., Islam, M. S., Coulson, R. L., Lopez, S. J., Ciernia, A. V., Chu, R. G., Yasui, D. H., Pessah, I. N., Lott, P., Mordaunt, C., et al. (2016). Cumulative impact of polychlorinated biphenyl and large chromosomal duplications on dna methylation, chromatin, and expression of autism candidate genes. *Cell reports*, 17(11):3035–3048.
- Efron, B. (1986). Double exponential families and their use in generalized linear regression. *Journal of the American Statistical Association*, 81(395):709–721.
- Elashoff, M. and Ryan, L. (2004). An em algorithm for estimating equations. *Journal of Computational and Graphical Statistics*, 13(1):48–65.
- Fan, J., Hu, J., Xue, C., Zhang, H., Susztak, K., Reilly, M. P., Xiao, R., and Li, M. (2020). Asep: Gene-based detection of allele-specific expression across individuals in a population by rna sequencing. *PLoS Genetics*, 16(5):e1008786.
- Farrington, C. (1995). Pearson statistics, goodness of fit, and overdispersion in generalised linear models. In *Statistical Modelling*, pages 109–116. Springer.
- Feinberg, A. P. (2007). Phenotypic plasticity and the epigenetics of human disease. *Nature*, 447(7143):433.

- Feng, H., Conneely, K. N., and Wu, H. (2014). A bayesian hierarchical model to detect differentially methylated loci from single nucleotide resolution sequencing data. *Nucleic acids research*, 42(8):e69–e69.
- Fletcher, D. (2012). Estimating overdispersion when fitting a generalized linear model to sparse data. *Biometrika*, 99(1):230–237.
- Forslind, K., Ahlmén, M., Eberhardt, K., Hafström, I., and Svensson, B. (2004). Prediction of radiological outcome in early rheumatoid arthritis in clinical practice: role of antibodies to citrullinated peptides (anti-ccp). *Annals of the rheumatic diseases*, 63(9):1090–1095.
- Goeman, J. J., Van De Geer, S. A., and Van Houwelingen, H. C. (2006). Testing against a high dimensional alternative. *Journal of the Royal Statistical Society: Series B (Statistical Methodology)*, 68(3):477–493.
- Hansen, K. D., Langmead, B., and Irizarry, R. A. (2012). Bsmooth: from whole genome bisulfite sequencing reads to differentially methylated regions. *Genome biology*, 13(10):R83.
- Hansen, K. D., Timp, W., Bravo, H. C., Sabunciyan, S., Langmead, B., McDonald, O. G., Wen, B., Wu, H., Liu, Y., Diep, D., et al. (2011). Increased methylation variation in epigenetic domains across cancer types. *Nature genetics*, 43(8):768.
- Hanson, M. A. and Gluckman, P. D. (2008). Developmental origins of health and disease: new insights. *Basic & clinical pharmacology & toxicology*, 102(2):90–93.
- Hebestreit, K., Dugas, M., and Klein, H.-U. (2013). Detection of significantly differentially methylated regions in targeted bisulfite sequencing data. *Bioinformatics*, 29(13):1647–1653.
- Heyde, C. and Morton, R. (1996). Quasi-likelihood and generalizing the em algorithm. *Journal of the Royal Statistical Society: Series B (Methodological)*, 58(2):317–327.
- Horvath, S. (2013). Dna methylation age of human tissues and cell types. *Genome biology*, 14(10):3156.

- Hu, M., Yao, J., Cai, L., Bachman, K. E., Van Den Brûle, F., Velculescu, V., and Polyak, K. (2005). Distinct epigenetic changes in the stromal cells of breast cancers. *Nature genetics*, 37(8):899–905.
- Hudson, M., Bernatsky, S., Colmegna, I., Lora, M., Pastinen, T., Klein Oros, K., and Greenwood, C. M. (2017). Novel insights into systemic autoimmune rheumatic diseases using shared molecular signatures and an integrative analysis. *Epigenetics*, 12(6):433–440.
- Ivanova, A., Molenberghs, G., and Verbeke, G. (2014). A model for overdispersed hierarchical ordinal data. *Statistical Modelling*, 14(5):399–415.
- Jaenisch, R. and Bird, A. (2003). Epigenetic regulation of gene expression: how the genome integrates intrinsic and environmental signals. *Nature genetics*, 33:245.
- Johnson, N. L., Kotz, S., and Balakrishnan, N. (1995). *Continuous univariate distributions*. John Wiley & Sons, Ltd.
- Jones, P. A. (1999). The dna methylation paradox. *Trends in Genetics*, 15(1):34–37.
- Jørgensen, B. (1987). Exponential dispersion models. *Journal of the Royal Statistical Society: Series B (Methodological)*, 49(2):127–145.
- Kato, T., Iwamoto, K., Kakiuchi, C., Kuratomi, G., and Okazaki, Y. (2005). Genetic or epigenetic difference causing discordance between monozygotic twins as a clue to molecular basis of mental disorders. *Molecular psychiatry*, 10(7):622–630.
- Korthauer, K., Chakraborty, S., Benjamini, Y., and Irizarry, R. A. (2018). Detection and accurate false discovery rate control of differentially methylated regions from whole genome bisulfite sequencing. *Biostatistics*.
- Lakhal-Chaieb, L., Greenwood, C. M., Ouhourane, M., Zhao, K., Abdous, B., and Oualkacha, K. (2017). A smoothed em-algorithm for dna methylation profiles from sequencing-based methods in cell lines or for a single cell type. *Statistical applications in genetics and molecular biology*, 16(5-6):333–347.
- Lea, A. J., Tung, J., and Zhou, X. (2015). A flexible, efficient binomial mixed model for identifying differential dna methylation in bisulfite sequencing data. *PLoS genetics*, 11(11):e1005650.

- Leek, J. T., Scharpf, R. B., Bravo, H. C., Simcha, D., Langmead, B., Johnson, W. E., Geman, D., Baggerly, K., and Irizarry, R. A. (2010). Tackling the widespread and critical impact of batch effects in high-throughput data. *Nature Reviews Genetics*, 11(10):733–739.
- Lindsay, B. (1982). Conditional score functions: some optimality results. *Biometrika*, 69(3):503–512.
- Lister, R., Pelizzola, M., Dowen, R. H., Hawkins, R. D., Hon, G., Tonti-Filippini, J., Nery, J. R., Lee, L., Ye, Z., Ngo, Q.-M., et al. (2009). Human dna methylomes at base resolution show widespread epigenomic differences. *nature*, 462(7271):315.
- McCullagh, P. (1985). On the asymptotic distribution of pearson’s statistic in linear exponential-family models. *International Statistical Review/Revue Internationale de Statistique*, pages 61–67.
- McCullagh, P. and Nelder, J. A. (1989). Generalized linear models 2nd edition chapman and hall. *London, UK*.
- McGregor, K., Bernatsky, S., Colmegna, I., Hudson, M., Pastinen, T., Labbe, A., and Greenwood, C. M. (2016). An evaluation of methods correcting for cell-type heterogeneity in dna methylation studies. *Genome biology*, 17(1):84.
- McRae, A. F., Powell, J. E., Henders, A. K., Bowdler, L., Hemani, G., Shah, S., Painter, J. N., Martin, N. G., Visscher, P. M., and Montgomery, G. W. (2014). Contribution of genetic variation to transgenerational inheritance of dna methylation. *Genome biology*, 15(5):R73.
- Meaney, M. J. and Szyf, M. (2005). Environmental programming of stress responses through dna methylation: life at the interface between a dynamic environment and a fixed genome. *Dialogues in clinical neuroscience*, 7(2):103.
- Molenberghs, G., Verbeke, G., and Demétrio, C. G. (2007). An extended random-effects approach to modeling repeated, overdispersed count data. *Lifetime data analysis*, 13(4):513–531.
- Molenberghs, G., Verbeke, G., Demétrio, C. G., Vieira, A. M., et al. (2010). A family of generalized linear models for repeated measures with normal and conjugate random effects. *Statistical science*, 25(3):325–347.

- Molenberghs, G., Verbeke, G., Iddi, S., and Demétrio, C. G. (2012). A combined beta and normal random-effects model for repeated, overdispersed binary and binomial data. *Journal of Multivariate Analysis*, 111:94–109.
- Ober, C. and Vercelli, D. (2011). Gene–environment interactions in human disease: nuisance or opportunity? *Trends in genetics*, 27(3):107–115.
- Park, Y., Figueroa, M. E., Rozek, L. S., and Sartor, M. A. (2014). MethySig: a whole genome dna methylation analysis pipeline. *Bioinformatics*, 30(17):2414–2422.
- Park, Y. and Wu, H. (2016). Differential methylation analysis for bs-seq data under general experimental design. *Bioinformatics*, 32(10):1446–1453.
- Prochenka, A., Pokarowski, P., Gasperowicz, P., Kosińska, J., Stawiński, P., Zbieć-Piekarska, R., Spólnicka, M., Branicki, W., and Płoski, R. (2015). A cautionary note on using binary calls for analysis of dna methylation. *Bioinformatics*, 31(9):1519–1520.
- Rackham, O. J., Langley, S. R., Oates, T., Vradi, E., Harmston, N., Srivastava, P. K., Behmoaras, J., Dellaportas, P., Bottolo, L., and Petretto, E. (2017). A bayesian approach for analysis of whole-genome bisulphite sequencing data identifies disease-associated changes in dna methylation. *Genetics*, pages genetics–116.
- Schoofs, T., Rohde, C., Hebestreit, K., Klein, H.-U., Göllner, S., Schulze, I., Lerdrup, M., Dietrich, N., Agrawal-Singh, S., Witten, A., et al. (2013). Dna methylation changes are a late event in acute promyelocytic leukemia and coincide with loss of transcription factor binding. *Blood, The Journal of the American Society of Hematology*, 121(1):178–187.
- Shao, X., Hudson, M., Colmegna, I., Greenwood, C. M., Fritzler, M. J., Awadalla, P., Pastinen, T., and Bernatsky, S. (2019). Rheumatoid arthritis-relevant dna methylation changes identified in acpa-positive asymptomatic individuals using methylome capture sequencing. *Clinical epigenetics*, 11(1):110.
- Shokoohi, F., Stephens, D. A., Bourque, G., Pastinen, T., Greenwood, C. M., and Labbe, A. (2018). A hidden markov model for identifying differentially methylated sites in bisulfite sequencing data. *Biometrics*.

- Shun, Z. and McCullagh, P. (1995). Laplace approximation of high dimensional integrals. *Journal of the Royal Statistical Society: Series B (Methodological)*, 57(4):749–760.
- Silverman, B. W. (1985). Some aspects of the spline smoothing approach to non-parametric regression curve fitting. *Journal of the Royal Statistical Society: Series B (Methodological)*, 47(1):1–21.
- Sims, D., Sudbery, I., Ilott, N. E., Heger, A., and Ponting, C. P. (2014). Sequencing depth and coverage: key considerations in genomic analyses. *Nature Reviews Genetics*, 15(2):121–132.
- Small, C. G., Christopher, G., Wang, J., et al. (2003). *Numerical methods for non-linear estimating equations*, volume 29. Oxford University Press on Demand.
- Vahabi, N., Kazemnejad, A., and Datta, S. (2019). A joint overdispersed marginalized random-effects model for analyzing two or more longitudinal ordinal responses. *Statistical Methods in Medical Research*, 28(1):50–69.
- Wahba, G. (1983). Bayesian “confidence intervals” for the cross-validated smoothing spline. *Journal of the Royal Statistical Society: Series B (Methodological)*, 45(1):133–150.
- Wood, S. N. (2011). Fast stable restricted maximum likelihood and marginal likelihood estimation of semiparametric generalized linear models. *Journal of the Royal Statistical Society: Series B (Statistical Methodology)*, 73(1):3–36.
- Wood, S. N. (2013). On p-values for smooth components of an extended generalized additive model. *Biometrika*, 100(1):221–228.
- Wood, S. N. (2017). *Generalized additive models: an introduction with R*. CRC press.
- Wreczycka, K., Gosdschan, A., Yusuf, D., Gruening, B., Assenov, Y., and Akalin, A. (2017). Strategies for analyzing bisulfite sequencing data. *Journal of biotechnology*, 261:105–115.
- Wu, H., Xu, T., Feng, H., Chen, L., Li, B., Yao, B., Qin, Z., Jin, P., and Conneely, K. N. (2015). Detection of differentially methylated regions from whole-genome

bisulfite sequencing data without replicates. *Nucleic acids research*, 43(21):e141–e141.

Zhao, K., Oualkacha, K., Lakhali-Chaieb, L., Labbe, A., Klein, K., Ciampi, A., Hudson, M., Colmegna, I., Pastinen, T., Zhang, T., et al. (2020). A novel statistical method for modeling covariate effects in bisulfite sequencing derived measures of dna methylation. *Biometrics*.

Ziller, M. J., Gu, H., Müller, F., Donaghey, J., Tsai, L. T.-Y., Kohlbacher, O., De Jager, P. L., Rosen, E. D., Bennett, D. A., Bernstein, B. E., et al. (2013). Charting a dynamic dna methylation landscape of the human genome. *Nature*, 500(7463):477.

Ziller, M. J., Stamenova, E. K., Gu, H., Gnirke, A., and Meissner, A. (2016). Targeted bisulfite sequencing of the dynamic dna methylome. *Epigenetics & chromatin*, 9(1):1–9.

A Marginal interpretations for dSOMNiBUS

A.1 Marginal mean

The latent variable representation of the logistic mixed effect model in (1) is

$$S_{ijk}^* = \eta_{ij} + \epsilon_{ij} + u_i$$

$$S_{ijk} = \begin{cases} 1, & \text{if } S_{ijk}^* \geq 0 \\ 0, & \text{if } S_{ijk}^* < 0 \end{cases}$$

where S_{ijk}^* is the unobserved latent variable, $\eta_{ij} = \sum_{p=0}^P \beta_p(t_{ij})Z_{pi}$ is the linear predictor calculated from all the fixed effect, ϵ_{ij} are iid error terms following a logistic distribution, and u_i is the subject-specific random effect as defined in Section 2.1. In addition, the error term ϵ_{ij} and RE u_i are mutually independent. Specifically, the cumulative distribution function (cdf) for ϵ takes the form $g(x) = 1/(1 + \exp(-x))$. The calculation of marginal mean $\pi_{ij}^M = \mathbb{P}(\eta_{ij} + \epsilon_{ij} + u_i \geq 0)$ requires integration over the joint distribution of ϵ_{ij} and u_i , which has no closed-form solution. Instead, we

can approximate the logistic cdf $g(x)$ by a normal cdf (Johnson et al., 1995, p. 119), which will lead to a more analytically tractable solution. Specifically, we have

$$g(x) \approx \Phi(cx), \text{ with } c = \sqrt{3.41}/\pi,$$

where $\Phi(x)$ is the cdf of the standard normal distribution. For any x value, the maximum absolute difference of this approximation is 0.00948.

Therefore, we can approximately view ϵ_{ij} as a normal random variable, $\epsilon_{ij} \sim N(0, 1/c^2)$. Since ϵ_{ij} and u_i are independent, we have $\epsilon_{ij} + u_i \sim N(0, 1/c^2 + \sigma_0^2)$. The marginal mean can be thus derived as

$$\begin{aligned} \pi_{ij}^M &= \mathbb{P}(\epsilon_{ij} + u_i \geq -\eta_{ij}) = \mathbb{P}\left(\frac{\epsilon_{ij} + u_i}{\sqrt{1/c^2 + \sigma_0^2}} \geq \frac{-\eta_{ij}}{\sqrt{1/c^2 + \sigma_0^2}}\right) \\ &\approx \Phi\left(\frac{\eta_{ij}}{\sqrt{1/c^2 + \sigma_0^2}}\right) \approx g\left(\frac{\eta_{ij}}{\sqrt{1 + c^2\sigma_0^2}}\right) \end{aligned}$$

A.2 Marginal variance

We will use the mixed effect model formulation in (1) to derive the marginal variance. Using the law of total variance, the marginal variance of S_{ij} is the sum of two parts:

$$\begin{aligned} \text{Var}(S_{ij}) &= \mathbb{E}\{\text{Var}(S_{ij} | u_i)\} + \text{Var}\{\mathbb{E}(S_{ij} | u_i)\} \\ &= \phi X_{ij} \mathbb{E}\{\pi_{ij}(1 - \pi_{ij})\} + X_{ij}^2 \text{Var}(\pi_{ij}), \end{aligned} \quad (20)$$

where $\pi_{ij} = g(\eta_{ij} + u_i)$ is the conditional mean dependent on u_i . The exact closed-form formula does not exist for either $\mathbb{E}(\pi_{ij})$ or $\text{Var}(\pi_{ij})$. Nevertheless, we can work on the second-order Taylor expansion of π_{ij} around $u_i = 0$, i.e. $\pi_{ij} = g(\eta_{ij} + u_i) \approx g(\eta_{ij}) + g'(\eta_{ij})u_i + g''(\eta_{ij})u_i^2/2$. Thus, we have $\mathbb{E}(\pi_{ij}) \approx g(\eta_{ij}) + g''(\eta_{ij})\sigma_0^2/2$,

$$\begin{aligned} \text{Var}(\pi_{ij}) &\approx \mathbb{E}\left\{\left[g'(\eta_{ij})u_i + \frac{g''(\eta_{ij})}{2}(u_i^2 - \sigma_0^2)\right]^2\right\} \\ &= \sigma_0^2 [g'(\eta_{ij})]^2 + \frac{\sigma_0^4}{2} [g''(\eta_{ij})]^2, \end{aligned}$$

and $\mathbb{E}(\pi_{ij}^2) \approx \sigma_0^2 [g'(\eta_{ij})]^2 + \frac{\sigma_0^4}{2} [g''(\eta_{ij})]^2 + \left[g(\eta_{ij}) + \frac{g''(\eta_{ij})}{2}\sigma_0^2\right]^2$. Substituting the above approximations into (20) yields the results in equation (4).

B Estimate ϕ from the contaminated data

B.1 No exact expression available for the E step for ϕ

Once evaluated the integral in the quasi-deviance $d_{ij}(S_{ij}, \pi_{ij})$ (7), the estimating equation for ϕ takes the form

$$\begin{aligned} \nabla_{\phi} \text{Laplace}(\Theta, \phi; \mathcal{B}^{(s)}, \mathbf{S}) &= \frac{1}{\phi^2} \sum_{i,j} \int_{S_{ij}/X_{ij}}^{\pi_{ij}^{(s)}} \frac{S_{ij} - X_{ij}\pi_{ij}}{\pi_{ij}(1 - \pi_{ij})} d\pi_{ij} + f_2(\Theta, \phi; \mathcal{B}^{(s)}) \\ &= \frac{1}{\phi^2} \sum_{i,j} \left\{ (X_{ij} - S_{ij}) \log(1 - \pi_{ij}^{(s)}) + S_{ij} \log(\pi_{ij}^{(s)}) \right. \\ &\quad \left. - (X_{ij} - S_{ij}) \log(1 - S_{ij}/X_{ij}) - S_{ij} \log(S_{ij}/X_{ij}) \right\} + f_2(\Theta, \phi; \mathcal{B}^{(s)}). \end{aligned}$$

This estimating equation is not linear in terms of the unknown methylated counts \mathbf{S} . Thus, replacing S_{ij} by $\eta_{ij}^* = \mathbb{E}(S_{ij} | Y_{ij}; \mathcal{B}^*, \Theta^*)$ does not necessarily provide an accurate estimate for $\mathbb{E}_{\mathbf{S}|Y;\Theta^*,\mathcal{B}^*}(\nabla_{\phi} \text{Laplace}(\Theta, \phi; \mathcal{B}^{(s)}, \mathbf{S}))$, and the exact expression for this expectation is not readily available from the first two moments of the distribution of S_{ij} .

B.2 The relation between ϕ_{ij}^Y and ϕ

All the expectation and variance in this section are conditional on the values of random effects u_i . For notational simplicity, we drop u_i from all the derivations in this section.

The variance of Y_{ij} depends on its mean π_{ij}^Y as well as the joint probability $\mathbb{P}(Y_{ijk} = 1, Y_{ijk'} = 1)$, i.e. observing methylated signals at both the k^{th} and k'^{th} reads, where $k, k' = 1, 2, \dots, X_{ij}$ and $k \neq k'$:

$$\begin{aligned} \text{Var}(Y_{ij}) &= \mathbb{E}(Y_{ij}^2) - [\mathbb{E}(Y_{ij})]^2 = \mathbb{E} \left\{ \left(\sum_{k=1}^{X_{ij}} Y_{ijk} \right)^2 \right\} - X_{ij}^2 (\pi_{ij}^Y)^2 \\ &= \sum_{k=1}^{X_{ij}} \mathbb{E}(Y_{ijk}^2) + 2 \sum_{k=1}^{X_{ij}} \sum_{k'=1}^{k-1} \mathbb{E}(Y_{ijk} Y_{ijk'}) - X_{ij}^2 (\pi_{ij}^Y)^2 \\ &= X_{ij} \pi_{ij}^Y - X_{ij}^2 (\pi_{ij}^Y)^2 + 2 \sum_{k=1}^{X_{ij}} \sum_{k'=1}^{k-1} \mathbb{P}(Y_{ijk} = 1, Y_{ijk'} = 1). \quad (21) \end{aligned}$$

By the law of total probability, we have

$$\mathbb{P}(Y_{ijk} = Y_{ijk'} = 1) = \sum_{s_1=0}^1 \sum_{s_2=0}^1 \mathbb{P}(S_{ijk} = s_1, S_{ijk'} = s_2) \mathbb{P}(Y_{ijk} = Y_{ijk'} = 1 \mid S_{ijk} = s_1, S_{ijk'} = s_2).$$

Joint distribution of the bivariate outcomes $(S_{ijk}, S_{ijk'})$. Note that, under our assumed mean-variance relationship in (2), S_{ijk} and $S_{ijk'}$ are not necessarily independent. Define $a_{ijkk'} = \mathbb{P}(S_{ijk} = 1, S_{ijk'} = 1)$. The joint probability mass function of $(S_{ijk}, S_{ijk'})$ can be thus written as

$$\begin{aligned} \mathbb{P}(S_{ijk} = 1, S_{ijk'} = 1) &= a_{ijkk'} \\ \mathbb{P}(S_{ijk} = 1, S_{ijk'} = 0) &= \pi_{ij} - a_{ijkk'} \\ \mathbb{P}(S_{ijk} = 0, S_{ijk'} = 1) &= \pi_{ij} - a_{ijkk'} \\ \mathbb{P}(S_{ijk} = 0, S_{ijk'} = 0) &= 1 - 2\pi_{ij} + a_{ijkk'}. \end{aligned}$$

We now can write the probability of observing two methylated reads as

$$\mathbb{P}(Y_{ijk} = Y_{ijk'} = 1) = p_0^2(1 - 2\pi_{ij} + a_{ijkk'}) + 2p_0p_1(\pi_{ij} - a_{ijkk'}) + p_1^2a_{ijkk'}.$$

Here, we assume that given the true methylation states S_{ijk} and $S_{ijk'}$, the observed methylation states Y_{ijk} and $Y_{ijk'}$ are independent.

Derive the values of $a_{ijkk'}$. From first principle, we can express the variance of

$$S_{ij} = \sum_{k=1}^{X_{ij}} S_{ijk},$$

$$\begin{aligned} \text{Var}(S_{ij}) &= \sum_{k=1}^{X_{ij}} \text{Var}(S_{ijk}) + 2 \sum_{k=1}^{X_{ij}} \sum_{k'=1}^{k-1} \text{Cov}(S_{ijk}, S_{ijk'}) \\ &= X_{ij}\pi_{ij}(1 - \pi_{ij}) + 2 \sum_{k=1}^{X_{ij}} \sum_{k'=1}^{k-1} \mathbb{E}(S_{ijk}S_{ijk'}) - 2 \sum_{k=1}^{X_{ij}} \sum_{k'=1}^{k-1} \mathbb{E}(S_{ijk})\mathbb{E}(S_{ijk'}) \\ &= X_{ij}\pi_{ij}(1 - \pi_{ij}) + 2 \sum_{k=1}^{X_{ij}} \sum_{k'=1}^{k-1} \mathbb{P}(S_{ijk} = 1, S_{ijk'} = 1) - X_{ij}(X_{ij} - 1)\pi_{ij}^2 \\ &= X_{ij}\pi_{ij}(1 - \pi_{ij}) + 2 \sum_{k=1}^{X_{ij}} \sum_{k'=1}^{k-1} a_{ijkk'} - X_{ij}(X_{ij} - 1)\pi_{ij}^2. \end{aligned}$$

On the other hand, we have $\text{Var}(S_{ij}) = \phi X_{ij} \pi_{ij} (1 - \pi_{ij})$. Equating these two quantities gives

$$2 \sum_{k=1}^{X_{ij}} \sum_{k'=1}^{k-1} a_{ijkk'} = (\phi - 1) X_{ij} \pi_{ij} (1 - \pi_{ij}) + X_{ij} (X_{ij} - 1) \pi_{ij}^2$$

Derive $\text{Var}(Y_{ij})$ and ϕ_Y . Now, we can plug the expression of $\mathbb{P}(Y_{ijk} = Y_{ijk'} = 1)$ in (21) and write $\text{Var}(Y_{ij})$ in terms of ϕ

$$\begin{aligned} \text{Var}(Y_{ij}) &= X_{ij} \pi_{ij}^Y - X_{ij}^2 (\pi_{ij}^Y)^2 + 2 \sum_{k=1}^{X_{ij}} \sum_{k'=1}^{k-1} [p_0^2 (1 - 2\pi_{ij} + a_{ijkk'}) + 2p_0 p_1 (\pi_{ij} - a_{ijkk'}) + p_1^2 a_{ijkk'}] \\ &= X_{ij} \pi_{ij}^Y - X_{ij}^2 (\pi_{ij}^Y)^2 + X_{ij} (X_{ij} - 1) \{p_0^2 (1 - 2\pi_{ij}) + 2p_0 p_1 \pi_{ij}\} + 2(p_0 - p_1)^2 \sum_{k=1}^{X_{ij}} \sum_{k'=1}^{k-1} a_{ijkk'} \\ &= X_{ij} \pi_{ij}^Y - X_{ij}^2 (\pi_{ij}^Y)^2 + X_{ij} (X_{ij} - 1) \{p_0^2 (1 - 2\pi_{ij}) + 2p_0 p_1 \pi_{ij}\} \\ &\quad + (p_0 - p_1)^2 \{(\phi - 1) X_{ij} \pi_{ij} (1 - \pi_{ij}) + X_{ij} (X_{ij} - 1) \pi_{ij}^2\} \\ &= X_{ij} \pi_{ij}^Y (1 - \pi_{ij}^Y) + (p_0 - p_1)^2 (\phi - 1) X_{ij} \pi_{ij} (1 - \pi_{ij}) \end{aligned}$$

The multiplicative dispersion parameter for the mis-measured outcome Y is thus

$$\phi_{ij}^Y = \frac{\text{Var}(Y_{ij})}{X_{ij} \pi_{ij}^Y (1 - \pi_{ij}^Y)} = 1 + (\phi - 1) \frac{\pi_{ij} (1 - \pi_{ij})}{\pi_{ij}^Y (1 - \pi_{ij}^Y)} (p_0 - p_1)^2.$$

Plugging in $\pi_{ij} = \frac{\pi_{ij}^Y - p_0}{p_1 - p_0}$ leads to the relation in (17).